

REPORT DOCUMENTATION PAGE

Form Approved
OMB No. 0704-0188

The public reporting burden for this collection of information is estimated to average 1 hour per response, including the time for reviewing instructions, searching existing data sources, gathering and maintaining the data needed, and completing and reviewing the collection of information. Send comments regarding this burden estimate or any other aspect of this collection of information, including suggestions for reducing the burden, to the Department of Defense, Executive Services and Communications Directorate (0704-0188). Respondents should be aware that notwithstanding any other provision of law, no person shall be subject to any penalty for failing to comply with a collection of information if it does not display a currently valid OMB control number.

PLEASE DO NOT RETURN YOUR FORM TO THE ABOVE ORGANIZATION.

1. REPORT DATE (DD-MM-YYYY) 30/06/2006		2. REPORT TYPE FINAL		3. DATES COVERED (From - To) Apr 2003 - Apr 2006	
4. TITLE AND SUBTITLE EXPERIMENTS IN NUMERICAL STUDIES OF LOW DENSITY AND REAL GAS EFFECTS ON REGIONS OF SHOCK WAVE/BOUNDARY LAYER INTERACTION IN HYPERVELOCITY FLOWS				5a. CONTRACT NUMBER F49620-03-1-0237	
				5b. GRANT NUMBER	
				5c. PROGRAM ELEMENT NUMBER	
				5d. PROJECT NUMBER	
				5e. TASK NUMBER	
				5f. WORK UNIT NUMBER	
6. AUTHOR(S) Michael S. Holden Timothy P. Wadhams Matthew MacLean Ronald A. Parker					
7. PERFORMING ORGANIZATION NAME(S) AND ADDRESS(ES) CUBRC 4455 Genesee Street Buffalo, NY 14225				8. PERFORMING ORGANIZATION REPORT NUMBER A-06-U-006	
9. SPONSORING/MONITORING AGENCY NAME(S) AND ADDRESS(ES) Air Force Office of Scientific Research 875 N. Randolph Street, Room 3112 Arlington, VA 22203-1954				10. SPONSOR/MONITOR'S ACRONYM(S) USAF, AFRL	
12. DISTRIBUTION/AVAILABILITY STATEMENT Approved for public release; distribution is unlimited				11. SPONSOR/MONITOR'S REPORT NUMBER(S) AFRL-SR-AR-TR-06-0285	
13. SUPPLEMENTARY NOTES					
14. ABSTRACT Experiments with extensive numerical simulations were conducted examining effects of low density flows and real gas effects on aerothermal characteristics of flows in hypervelocity facilities and in simple & complex flowfields in hypervelocity flows. These studies demonstrated that in the absence of real gas effects the DSMC & Navier-Stokes solutions accounting for slip effects were in excellent agreement with measurements. An extensive series of calibration and validation studies were done defining the free stream flows in the LENS I and X tunnels for low density and high enthalpy flows at velocities up to 16,000 ft/s. Measurements on double cone configuration showed that above 13,000 ft/s the interaction regions differed significantly in nitrogen and air flows; while the computations agreed with the measurements in nitrogen, they differed significantly in the size and properties of interaction regions in air. With the shuttle configuration, we demonstrated that real gas effects decrease the size of a separated interaction region over the flap, reduce the pressure over the adjacent curved surfaces, and reduce Reynolds number for onset of boundary layer transition.					
15. SUBJECT TERMS Real Gas Chemistry, Low Density Effects, Hypervelocity Flows, Boundary Layer Transition, Shock Wave/Boundary Layer Interaction, Separated Flows, Shock Tunnels, Expansion Tunnels, Laser Diagnostics, Code Validation, Navier-Stokes Solutions, DSMC Solutions					
16. SECURITY CLASSIFICATION OF:			17. LIMITATION OF ABSTRACT	18. NUMBER OF PAGES 69	19a. NAME OF RESPONSIBLE PERSON Dr. Michael S. Holden
a. REPORT U	b. ABSTRACT U	c. THIS PAGE U			19b. TELEPHONE NUMBER (Include area code) 716-631-6853



**4455 Genesee Street
Buffalo, New York 14225**

**EXPERIMENTS IN NUMERICAL STUDIES OF LOW DENSITY AND
REAL GAS EFFECTS ON REGIONS OF SHOCK WAVE/BOUNDARY
LAYER INTERACTION IN HYPERVELOCITY FLOWS**

AFOSR Contract No. F49620-03-1-0237

Final Report A06-U-006

Prepared for:

**United States Air Force
Dr. John Schmisser
AFOSR/NA
875 N. Randolph Street, Rm 3112
Arlington, VA 22203-1954**

Prepared by:

**Michael S. Holden
Timothy P. Wadhams
Matthew MacLean
Ronald A. Parker
Aerothermal Aero-Optic Evaluation Center (AAEC)**



20060816078

EXPERIMENTS IN NUMERICAL STUDIES OF LOW DENSITY AND REAL GAS EFFECTS ON REGIONS OF SHOCK WAVE/BOUNDARY LAYER INTERACTION IN HYPERVELOCITY FLOWS

AFOSR Grant No. F49620-03-1-0237

Michael S. Holden
Timothy Wadhams
Matthew MacLean
Ronald Parker
Aerothermal Aero-optic Evaluation Center (AAEC)
4455 Genesee Street
Buffalo, NY 14225

June 2006

Summary

In this program experimental studies supported by extensive numerical simulations were conducted to examine the effects of low density flows and real gas effects on the aerothermal characteristics of the flows in hypervelocity facilities and in simple and complex flowfields in hypervelocity flows. Following the earlier code validation studies to examine shock wave and shock/shock boundary layer interactions in laminar hypersonic nitrogen flows over the hollow cylinder/flare and double cone configurations, a series of studies were conducted at low Reynolds numbers to provide measurements with which to examine the performance of modified Navier-Stokes and DSMC methods to accurately compute the complex regions of shock boundary layer and shock/shock interaction over these models in low density flows. These studies demonstrated that in the absence of real gas effects the DSMC solutions, and Navier-Stokes solutions accounting for slip effects, were in excellent agreement with the measurements. The remainder of the program focused on experimental and numerical studies to examine real gas effects on facility flows and the flows over simple and complex body shapes, with the latter configurations designed to generate complex regions of laminar, shock/shock and shock/boundary layer interactions. The experimental studies were conducted in the LENS I shock tunnel and LENS X expansion tunnel. An extensive series of calibration and validation studies were performed to define the freestream flows in the LENS I tunnel for low density flows and high enthalpy flows at velocities up to 16,000 ft/s. Also preliminary studies were conducted to investigate the flows in the newly constructed LENS X expansion tunnel where again the experimental studies were supported with extensive numerical simulations. In both the LENS I and LENS X facility measurements were made to examine real gas effects over simple cylindrical, spherical, and conical nose shapes. Also, a major study was conducted to develop and employ laser diagnostics to measure the velocity and concentrations of NO and oxygen in the air stream. These measurements together with measurements on the walls of the nozzles were conducted to evaluate the chemical modeling employed in Navier-Stokes solutions for the nozzle flows. It was observed that in high enthalpy flows ($V \sim 14,000$ ft/s) that while the measurements of velocity were in good agreement with prediction, the measurements of NO concentration

(~ 2% to 3%) were significantly less than the predicted values (~6%). The measurements on the double cone configuration in air and nitrogen flows demonstrated that while there was little effect of real gas chemistry on the structure of the interaction regions at velocities below 10,000 ft/s, at velocities above 13,000 ft/s there were significant differences between the interaction regions in nitrogen and air flows. While the computations agreed with the measurements in nitrogen at the higher velocities, they differed significantly both in the size and properties of the interaction regions in air flow at velocities above 13,000 ft/s. The studies with the double cone configuration were followed by a major experimental program to evaluate real gas effects over a shuttle configuration. Here the major emphasis was on examining the real gas effects on the separated regions induced by shock wave/boundary layer interaction over the control surfaces, and in the expansion regions over the curved surfaces at the rear of the shuttle. These studies again demonstrated that real gas effects decrease the size of the interaction region over the flap control surface, in fact increasing its effectiveness. However, we observed that flow over the adjacent curved surfaces was influenced by flow chemistry with a reduction in pressure relative to the flow without significant dissociation, causing the pressures on the adjacent curved section of the wing to be lower because of nonequilibrium effects in the freestream. In these studies it was also observed that real gas chemistry can have a significant destabilizing effect on boundary layer transition, resulting in boundary layer and shear layers which become transitional or turbulent at lower Reynolds numbers than observed for flows in the absence of chemistry.

TABLE OF CONTENTS

	<u>Page No.</u>
Introduction	4
Calibration and Validation of the LENS I Shock Tunnel and LENS X Expansion Tunnel to Perform Experimental Studies in Low Density and High Enthalpy Flows	11
Introduction	
Calibration and validation of the flows in the LENS I reflected shock Tunnel at low density and high enthalpy conditions	
Laser Diode Measurements of Nonequilibrium Effects in Facility Air Flow	21
Introduction	
Experimental Setup and Optical Interface	
QCL Laser Spectrometer	
Summary of Results	
Preliminary Studies to Calibrate and Validate the LENS X Expansion Tunnel	28
Measurements in Low Density Flows on the Hollow Cylinder/Flare and Double Cone Configurations and Comparisons with Improved Navier-Stokes and DSMC Prediction Methods	34
Introduction	
Studies with the Hollow Cylinder/Flare Configuration	
Studies with the Double Cone Configuration	
Studies of Real Gas Effects in High Enthalpy Flows for Facility and Code Validation	41
Introduction	
Real Gas Effects in Hypervelocity Nitrogen, Air and Carbon Dioxide Flows On Simple Nose Shapes	
Measurements of Real Gas Effects on the Double Cone Configuration in the LENS I Shock Tunnel and LENS X Expansion Tunnel	46
Introduction	
Studies of Real Gas Effects on Regions of Separated Flow and Shock/ Shock Interaction on the Double Cone Configuration in LENS I	
Measurements in the LENS X Facility on the Double Cone Model	53
Introduction	
Measurements on the Double Cone Configuration in LENS X	
Navier-Stokes Predictions of Real Gas Effects and Comparison with Experiments	56
Preliminary Results of Studies of Real Gas Effects on Regions of Viscous/Inviscid Interaction on a NASA Space Shuttle Configuration	59
Introduction	
Models, Instrumentation and Test Conditions Employed in the Experimental Studies	
Results and Discussion	
Conclusions	65
References	66

INTRODUCTION

Even after a period of 25 years from when it was postulated that the aerodynamic control problems encountered during the first shuttle flight (STS-1) resulting from real gas and viscous interaction effects, and can significantly influence the stability and aerothermal loads on vehicles traveling at velocities above 12,000 ft/s, definitive sets of measurements are yet to be made to validate these suggestions. (Ref. 1). The design of new capsules for interplanetary flight as well as maneuvering re-entry vehicles and high-speed interceptors will rely on computer codes to predict real gas effects on the stability of the vehicle, the occurrence of boundary layer transition, and the characteristics of the regions of shock wave/boundary layer interaction. Even the most recent codes incorporating the most sophisticated chemistry models have yet to be directly validated for conditions above Mach 10 by direct comparison with experimental data. Recent studies by ESA with the Apollo capsule as well as DoD studies of maneuvering re-entry vehicles (Figure 1) have again demonstrated that we lack the ability to accurately predict real gas plasmas and their effects on boundary layer transition and vehicle stability at Mach 14 and above.

The problems with the control characteristics of the first flight of the U.S. Space Shuttle during its entry into the atmosphere (Figure 2) highlighted the importance of understanding and predicting the combined effects of viscous/inviscid interaction and flow chemistry effects in the laminar, high temperature hypervelocity flow regime. The inability to predict the pitch and moment characteristics of the shuttle has been attributed in part to the inability of ground test capabilities to simulate, and design methods to accurately assess, the decrease in flap effectiveness resulting from viscous/inviscid interaction and the effects of flowfield chemistry on the pressures over the flaps and on the curved adjacent surfaces (Figure 3). Explanations of the "shuttle anomaly" have relied heavily on numerical computations and, to a lesser extent testing in CF₄, to explain the differences between ground test measurements and flight test performance. However, models of flowfield air chemistry in this high-temperature flow regime, where temperatures in the shock layer are large enough to cause dissociation of both the oxygen and nitrogen molecules (see Figure 4), have not been validated directly at conditions where a decrease in control effectiveness was observed. Likewise testing in a gas with a fixed lower specific heat ratio (γ) (see Figure 5) has very limited application to simulate the non-equilibrium relaxation processes that occur on vehicles entering the atmosphere at above 5 km/sec. While significant advances have been made in the accuracy and robustness of numerical codes, the advancements in the understanding and modeling of flowfield chemistry since the design of the shuttle have been relatively small and there have been no systematic studies, either experimental or numerical, to validate them.

The experimental studies of real gas effects on vehicle aerothermodynamics presented in this report build on our preliminary research to investigate nonequilibrium chemistry effects in 14 kft/sec air flow over a blunted cone/flare configuration (Ref. 2), studies at similar velocities over a 25°/60° double cone configuration, and measurements in Type IV shock/shock interaction regions (Ref. 3). Although significant nonequilibrium air chemistry was generated over the blunted cone/flare model (see Figure 6), comparisons between the measurements and predictions shown in Figure 7 indicate that boundary layer transition, which occurred at the cone/flare junction, masked any effects resulting from flowfield chemistry. Measurements in nitrogen and air in regions of shock/boundary layer and shock/shock interaction over a 25°/60° double cone configuration and shock interaction models respectively, did not provide definitive evidence to

evaluate real gas effects. Comparisons between the measurements on the double cone configuration (shown in Figure 8a) and Candler's unsteady solutions to the Navier-Stokes equations are shown in Figures 8b and 8c. While both theory and experiment indicate significant real gas effects, the computed results were unsteady while measurements indicated the flow was steady. Comparisons between numerical prediction and experiments for Type IV shock/ shock interaction on a cylindrical leading edge (see Figure 9a) in high enthalpy flows shown in Figures 9b and 9c again produced inconclusive results.

Based on our earlier results (Ref. 2), it was clear that to provide measurements of code validation quality, detailed experimental measurements in well-defined interaction regions with air and nitrogen freestreams over simple and complex models were required. Our more recent studies with the 25°/55° double cone configuration demonstrated that this configuration provides one of the most suitable models for code validation studies. The facility calibration studies conducted during this program in both air and nitrogen flows employed nozzle and freestream measurements, coupled with detailed numerical simulations of the flows in the reservoir, nozzle and test section of the tunnel, and have provided us with a rational procedure for computing non-equilibrium freestream conditions. The addition of the LENS X expansion tunnel has also provided us with the potential to generate hypervelocity flows in the absence of freestream dissociation.

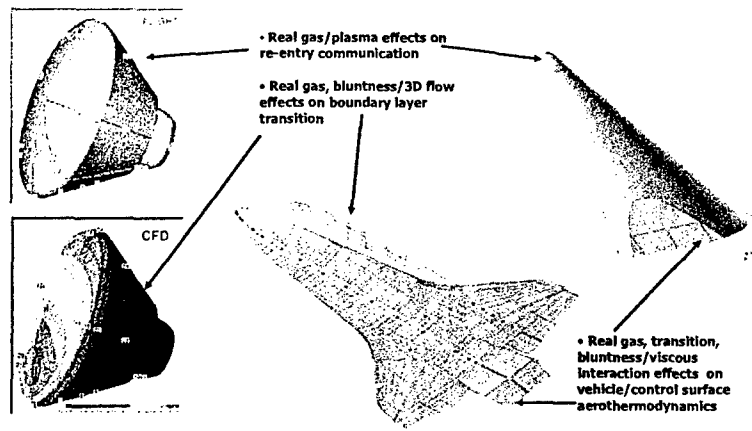


Figure 1 Real Gas and Boundary Layer Transition Effects on Blunt and Slender Re-entry Vehicles

STS-1 Shuttle Hypersonic Pitch Trim Anomaly

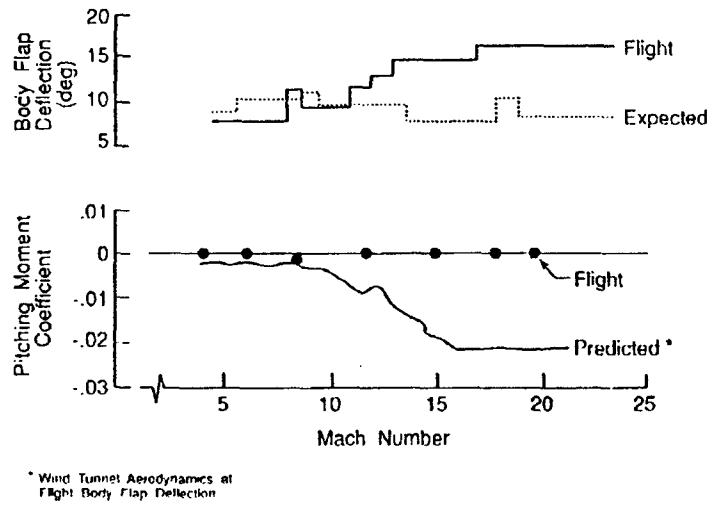


Figure 2 STS-1 Shuttle Hypersonic Pitch Trim Anomaly

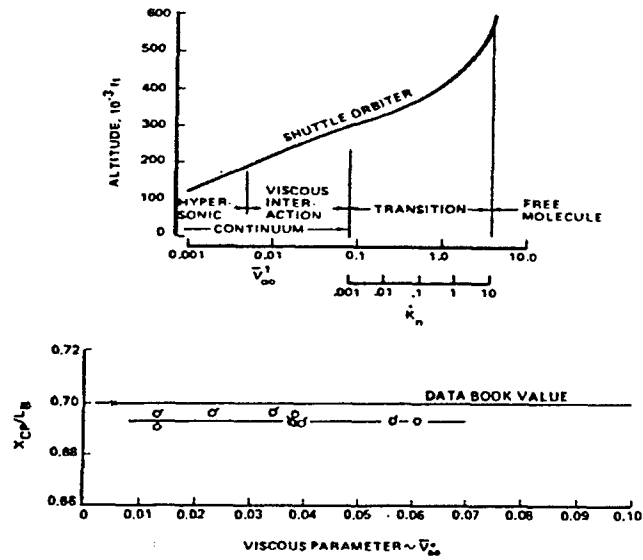


Figure 3 Measurements Demonstrating Low Density Viscous Interaction Effects on Shuttle Stability

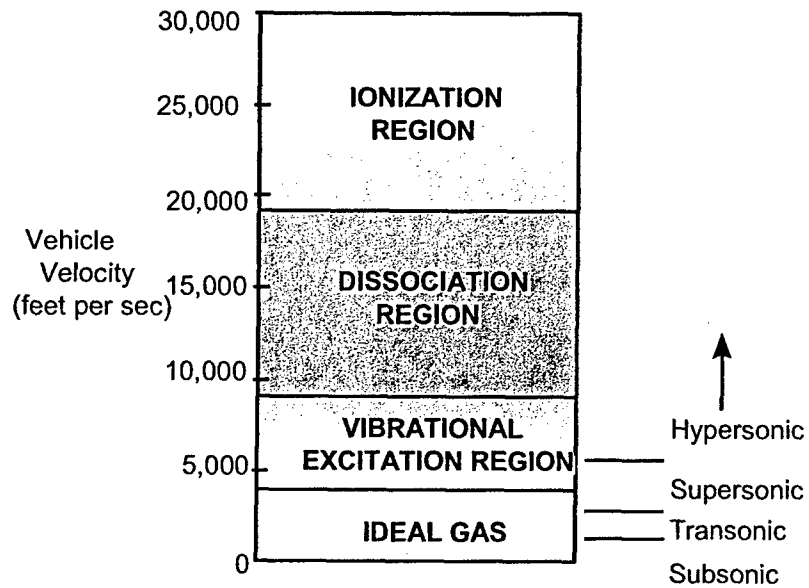


Figure 4 Real Gas Chemistry Effects in Hypervelocity Flows

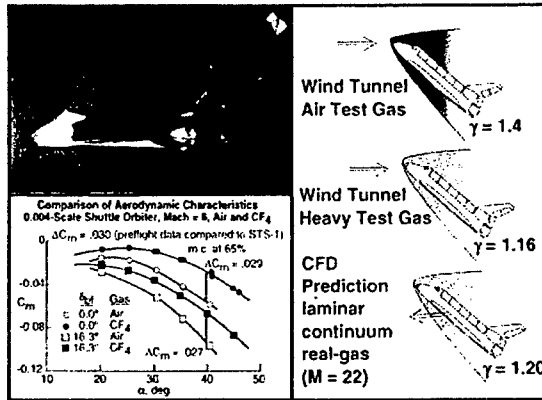


Figure 5 Pitching Moment Measurements from Tests in CF4 Indicating Real Gas Effects

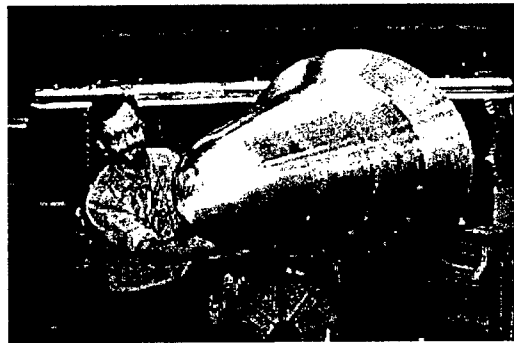


Figure 6 Spherically Blunted Cone/Flare Configuration Employed in Studies to Examine Real Gas Effects (Ref. 19)

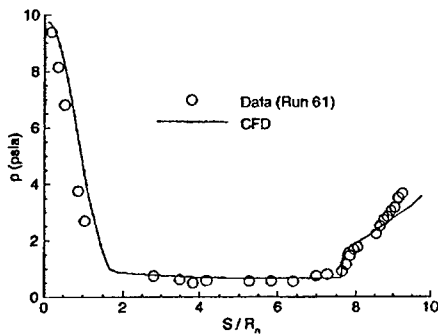


Figure 7a Comparison between Navier-Stokes Code Calculations and Pressure Measurements over Blunted Cone/Flare Configuration

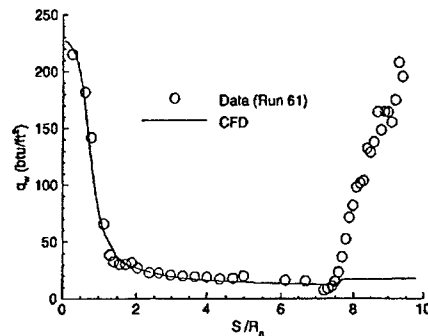
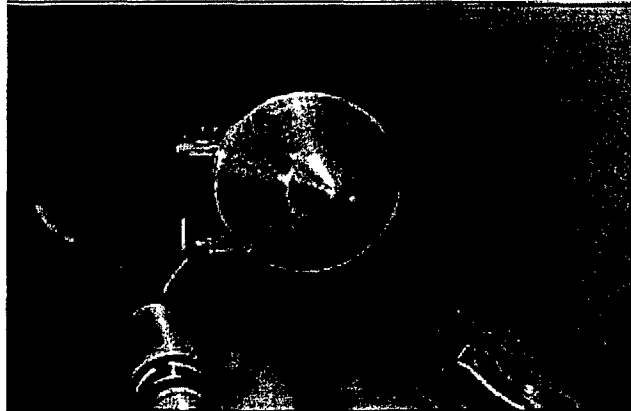
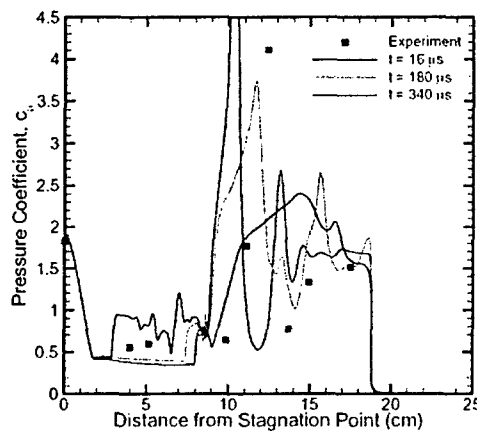


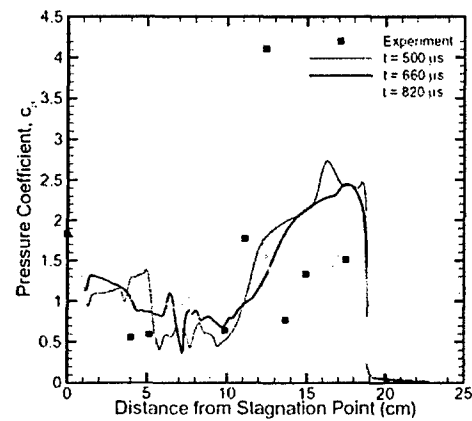
Figure 7b Comparison between Navier-Stokes Code Calculations and Heat Transfer Measurements over Blunted Cone/Flare Configuration



(a) Photograph of Double Cone Model Used in Earlier Real Gas Studies

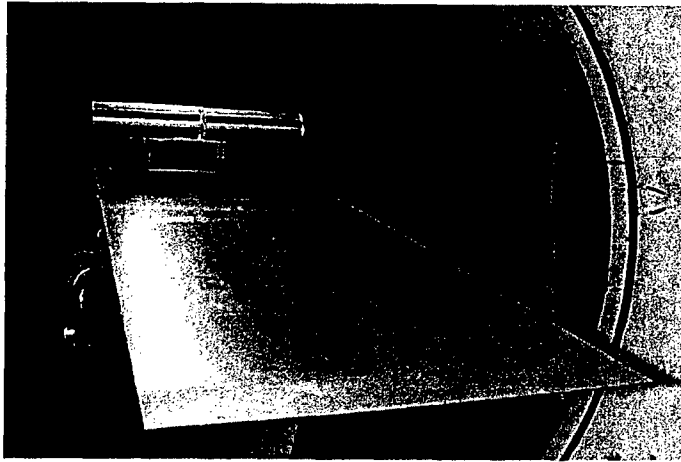


(b) Nitrogen

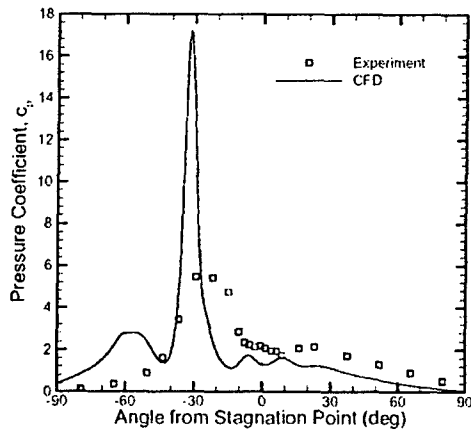


(c) Air

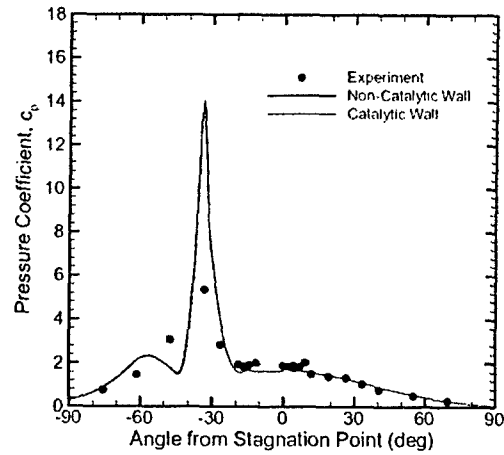
Figure 8 Comparisons between Navier Stokes Predictions and Measurements in Air and Nitrogen over $25^\circ/60^\circ$ Double Cone Configuration (Candler, Ref. 4)



(a) Photograph of Shock/Shock Interaction Model



(b) Run 48 Conditions (10.5 MJ/kg Nitrogen)



(c) Run 50 Conditions (11.3 MJ/kg Air)

Figure 9 Comparisons between Surface Measurements and Computation in Shock/Shock Interaction Regions in Nitrogen and Air (Ref. 4)

CALIBRATION AND VALIDATION OF THE LENS I SHOCK TUNNEL AND LENS X EXPANSION TUNNEL TO PERFORM EXPERIMENTAL STUDIES IN LOW DENSITY AND HIGH ENTHALPY FLOWS

Introduction

A major part of the program to evaluate low density and real gas effects on the aerothermal characteristics of vehicles designed to fly at hypersonic speeds was an experimental program to investigate and validate the characteristics of the ground test facilities we employed to generate low density and high enthalpy flows. In this program, we employed the LENS I and LENS X test facilities to generate velocities between 7,000 and 16,000 ft/s in nitrogen, air and CO₂ flows. The LENS I facility is a reflected shock tunnel where a reservoir of high temperature, high pressure gas is generated by reflecting a strong shock from the endwall of the tunnel. In this reservoir region, the gas reaches temperatures up to 10,000°K resulting in significant vibration and dissociation effects which can persist as the flow is expanded into the test section of the tunnel. It is of key importance to know the level of the nonequilibrium flow chemistry in the test section as well as to accurately predict these flows. The LENS X facility is an expansion tunnel where the flow is both heated and compressed initially with a shock wave and then energy added employing an unsteady expansion so that with the correct set of initial conditions the flow entering the test section can have little or no real gas chemistry. Generally the drawbacks of the expansion tunnel are very short test times (of the order of ~ 50 μs); however the LENS X facility is so large that test times up to 3 msec can be generated. The LENS X facility was constructed during this program (with other funding) and calibration was performed to investigate and validate the flows at the end of the expansion section upstream of the nozzle and in the test section of the tunnel. A major advantage of employing the two facilities is by testing in the LENS I and LENS X at the same velocity we can examine real gas effects over the model with different levels of nonequilibrium in the freestream.

The calibration/validation studies performed in the LENS I and X tunnels consisted of measurements in the reservoir and test sections of the tunnels with conventional wall and freestream intrusive probe assemblies as well as with the newly developed laser diode techniques. Because of the thermally stressing high enthalpy environment, these measurements are not simple to make, and significant instrumentation development was undertaken to obtain accurate measurements particularly for the heat transfer and pressure measurements in the small probes employed in our survey rakes. Also specialized experimental apparatus were constructed for the laser diode measurements to minimize extraneous effects associated with the shear flows at the edges of the nozzle flow.

As a key part of this work, numerical computations were performed with Candler's nozzle codes employing the most recent models of nonequilibrium flow chemistry and models for the development of the turbulent boundary layer in the strong favorable pressure gradient developed along the nozzle. The DPLR code as developed by Michael Wright of NASA/Ames was also employed extensively to calculate the nonequilibrium flows over both simple and complex model configurations.

Calibration and Validation of the Flows in the LENS I Reflected Shock Tunnel at Low Density and High Enthalpy Conditions

The LENS I and II are reflected shock tunnels (Ref. 5) with the capabilities of conducting tests from Mach 4 to 18 at altitudes down to sea level and up to over 80 km illustrated in the velocity/altitude map as shown in Figure 10. Figure 11 shows a photograph of the driven sections, nozzles, and test sections of the LENS I and II. The LENS I, shown schematically in Figure 12, is a reflected shock tunnel with an 8-inch diameter driven tube which is 90 ft in length. The heated driver section can be operated with mixtures of nitrogen, helium and hydrogen; a helium buffer gas is employed in the double-diaphragm valve. This tunnel can be operated under tailored interface conditions up to velocities of 15 kft/s. When operated at the 10 kft/s and 14 kft/s conditions, we obtain run times of 12 and 6 ms, respectively, giving over 200 flow lengths over the double cone model.

A major part of the current program was directed toward obtaining and establishing well-defined freestream conditions to provide accurate upstream conditions for the numerical simulations and the experimental correlations. Both experiment and Navier-Stokes computations were employed to generate the freestream conditions and the nonequilibrium test conditions were computed using a method developed in this program. Measurements were made across the exit plane of the tunnel using high-frequency pressure and thin film heat transfer instrumentation installed in pitot pressure and stagnation point heat transfer probes respectively. Measurements were also made with spherical, cylindrical and conical probes containing similar instrumentation. A photograph of the survey rake containing this instrumentation is shown in Figure 13. In addition to measurements with the survey rake, measurements were made in the driven tube and reservoir of the tunnel; and heat transfer measurements were made along the nozzle. A photograph showing the rays of heat transfer instrumentation in the nozzle and the survey rake is shown in Figure 14. The heat transfer measurements made along the nozzle for two major test cases are compared in Figure 15 with Navier-Stokes calculations where we selected the turbulence model which most effectively replicated the experimental data. Nozzle flow calculations were obtained with the selected turbulence model for a number of different models describing the nonequilibrium flow chemistry. These calculations are compared with the measured Mach number distribution in Figure 16. Again, the chemistry model which gave the best agreement with experiment over a large range of test conditions was selected to calculate the freestream conditions which were supplied to the computationalist and used to nondimensionalize the experimental data. To further validate our procedures for calculating test conditions, measurements were made around spherical nosetips and along the stagnation line of a circular cylinder (Figure 17).

During the tunnel calibration for the studies of low density flow, heat transfer measurements were made around hemispherical nosetips and along the stagnation line of a small circular cylinder to provide information with which to evaluate the performance of Navier-Stokes and DSMC prediction methods in high temperature, low density flows for Reynolds numbers down to values of 100 for the circular cylinder and 1,000 for the hemispherical nosetip. Two hemispherical nosetips were mounted in the survey rake (shown in Figure 17a) during the calibration studies. Figure 17b is an enlargement taken from Figure 17a showing the contoured thin-film heat transfer buttons which were installed around the hemispherical nosetip. We employed platinum thin-film gages both uncoated and coated with a silicon dioxide to provide catalytic and noncatalytic surfaces to investigate catalytic wall effects. This figure shows a

photograph of the 0.17-inch diameter cylinder instrumented with eight thin-film heat transfer gages along its centerline. Heat transfer measurements were obtained with this probe over a Reynolds number (based on cylinder diameter) from 100 to 1,000. Measurements were made on the hemispherical and cylindrical nosetips over a range of velocity and density freestream conditions to obtain flowfields which spanned the continuum to the fully merged rarefied flow regime. The comparison between the measured heat transfer distribution on the hemispherical nosetips and the results from the simple Fay Riddell prediction technique suggests that even down to Reynolds numbers of 1,000 (Figures 18 to 20) this simple prediction technique can be used with good accuracy. This is further illustrated in Figure 21, which is a compilation of all the measurements nondimensionalized by the Fay Riddell prediction, giving a value of close to 1 over the Reynolds number span at which the studies were conducted.

The measurements on the 0.175-inch diameter cylinder, however, indicate that at the very low Reynolds numbers at which the studies were conducted the heating rate drops below that predicted by Fay Riddell. Figure 22a shows distribution of heating across the cylinder for the 12 run conditions at which this study was conducted. Here it can be seen that the nondimensional heating varies between 1 and 0.8 depending on the freestream conditions. Plotting these measurements against the cylinder Reynolds number as shown in Figure 22b, we observe that for Reynolds numbers close to 1,000, the measurements are close to the Fay Riddell value. When the Reynolds number drops close to 100 there is a 20% decrease in the heating level. The consistency between the measurements with the coated and uncoated instrumentation indicated that for the test conditions at which these studies were conducted, surface catalysis did not have a significant influence on the stagnation heating value.

The studies summarized here were reported in AIAA Paper 2004-0916 and AIAA Paper 2004-0529.

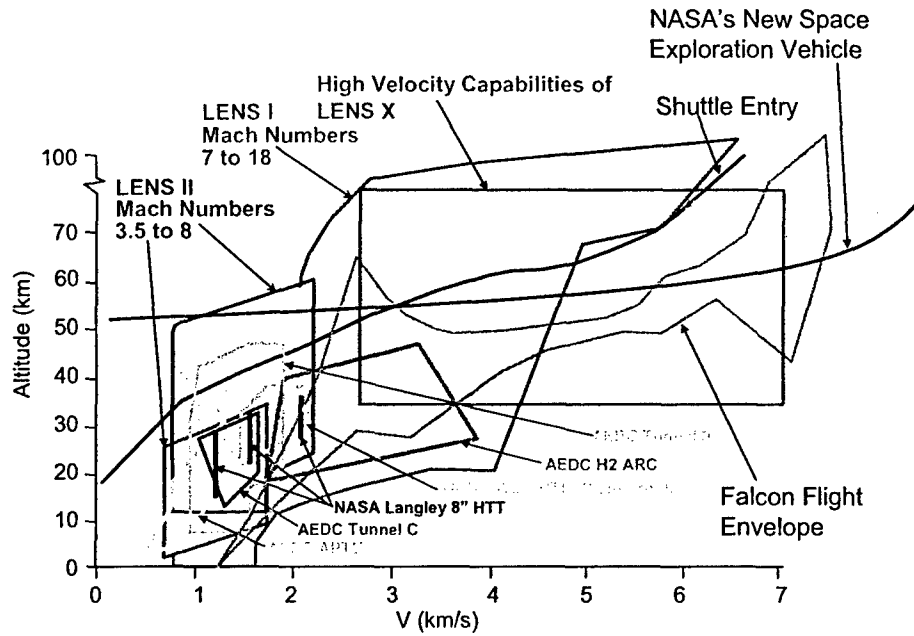


Figure 10 Velocity/Altitude Performance of the LENS I, II and X Test Facilities

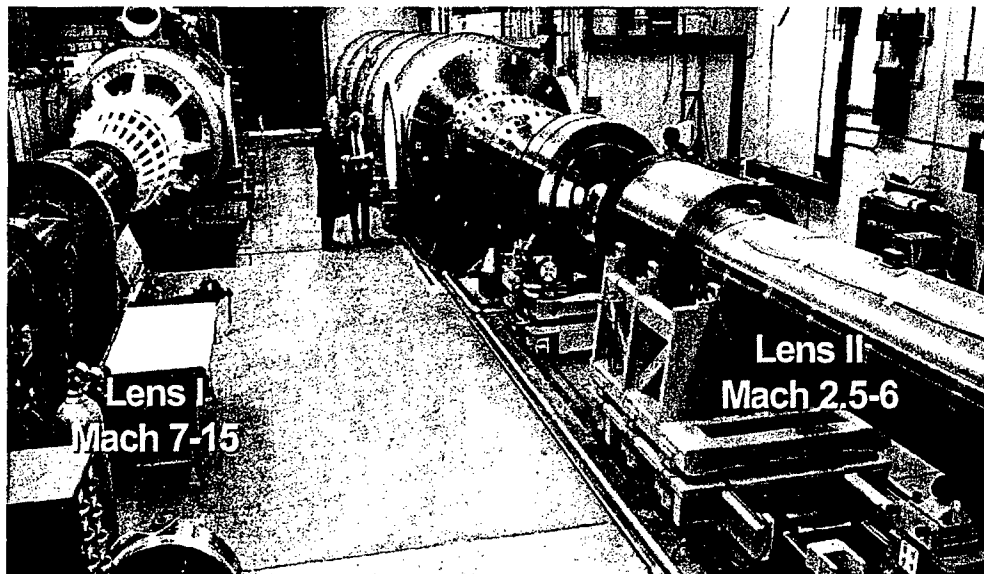


Figure 11 Photograph of the LENS I and II Reflected Shock Tunnels

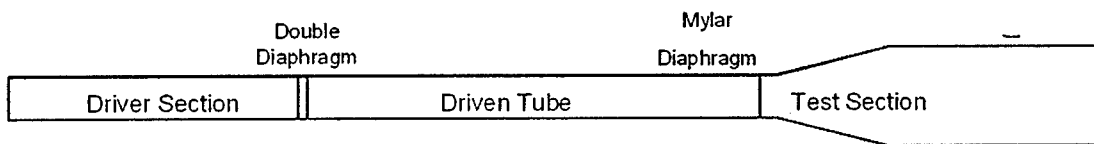
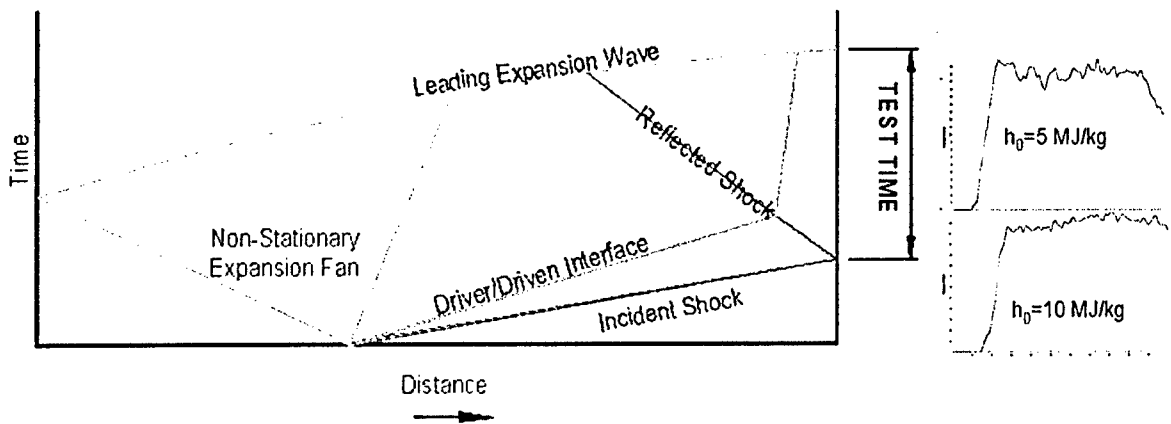
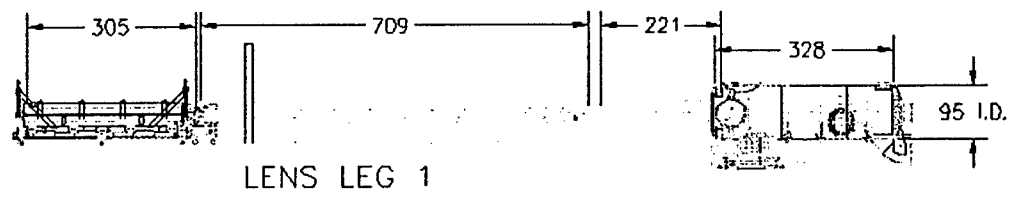


Figure 12 Tunnel Layout, Wave Diagram and Pitot Pressure Traces for LENS I

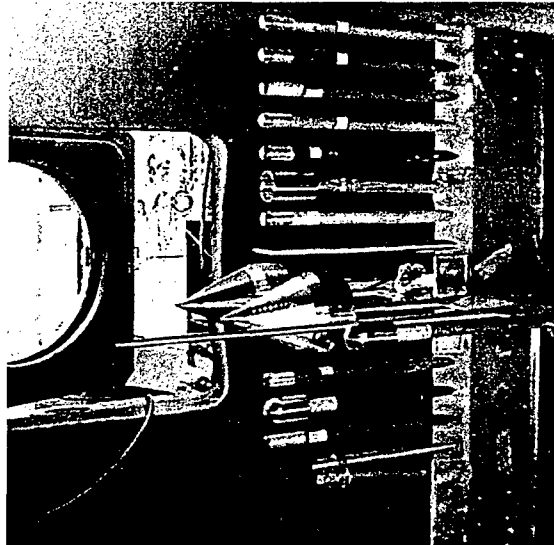


Figure 13 Survey Rake containing Instrumentation to Measure Pitot and Static Pressure, Heating Distributions on Cylinders and Spheres, and Cone Pressures and Heating

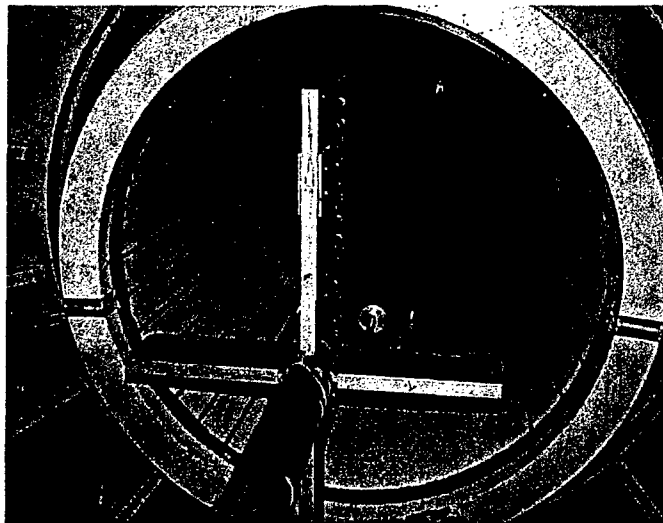


Figure 14 Photograph showing Instrumented Nozzle and Survey Rake Positioned in the Exit Plane of the Nozzle to Evaluate and Define Test Conditions

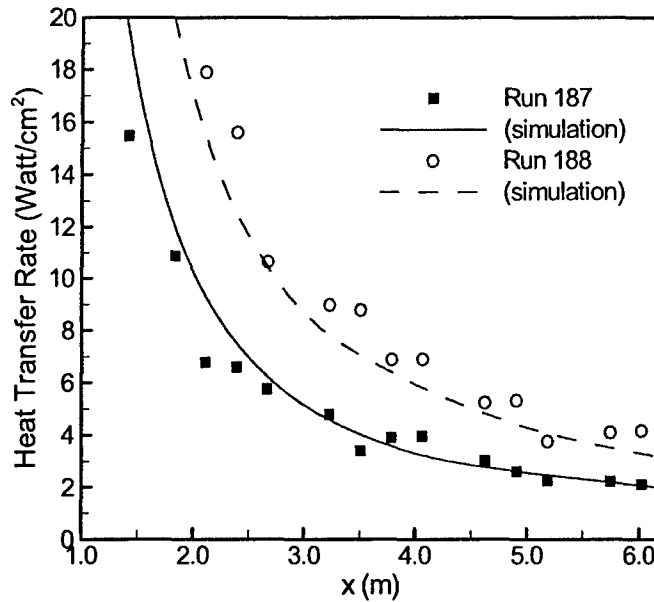


Figure 15 Comparisons between Navier-Stokes Predictions and Heat Transfer Measurements along the Contoured Nozzles for Two Test Conditions

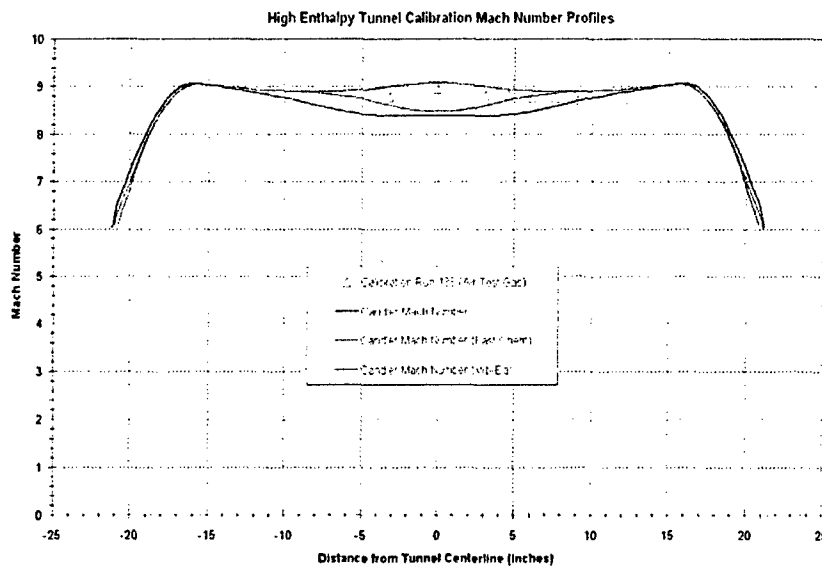
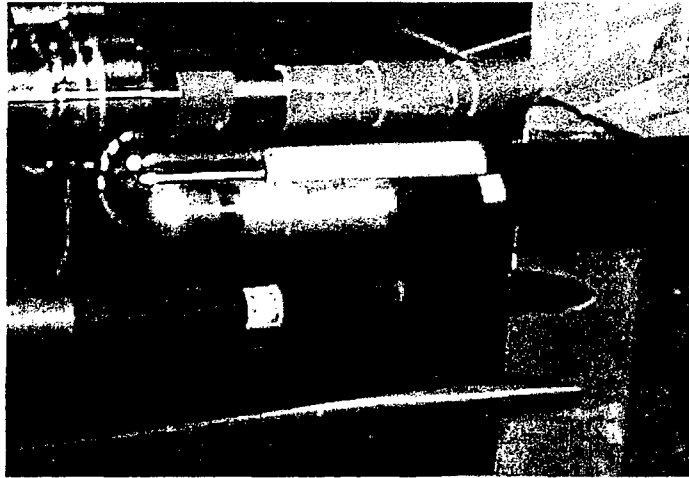


Figure 16 Comparisons between Measurements across the Exit Plane of the Nozzle and Navier-Stokes Computations with a Range of Chemistry Models to Evaluate and Calibrate the Numerical Codes



(a)



(b)

Figure 17 Hemispherical and Cylindrical Nosetips containing Thin-Film Heat Transfer Gages

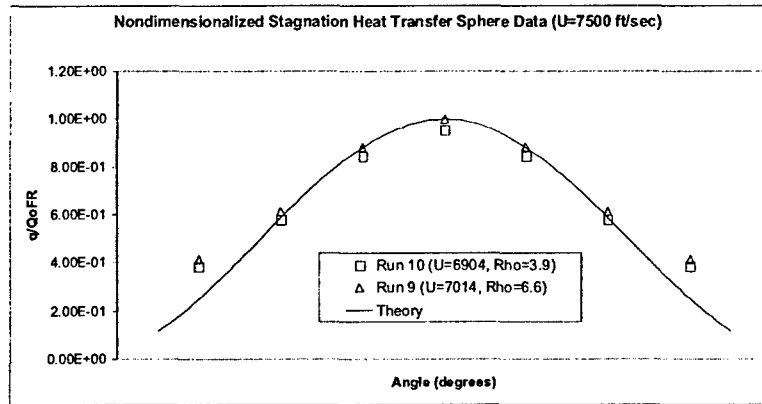


Figure 18 Comparison between Heat Transfer Measurements around a Hemispherical Noretip and Fay Riddell Predictions (U = 7,000 ft/s)

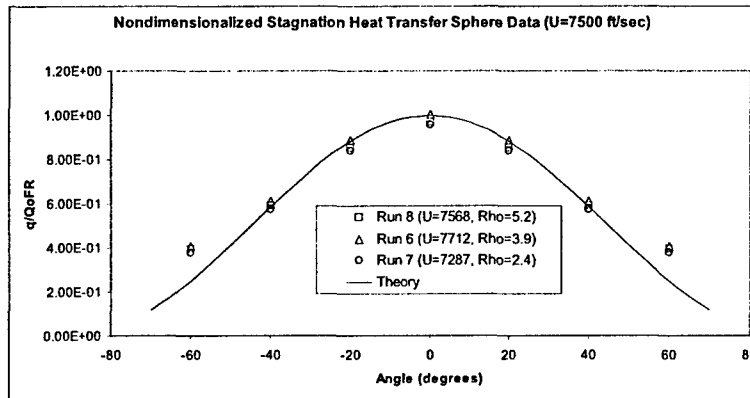


Figure 19 Comparison between Heat Transfer Measurements around a Hemispherical Noretip and Fay Riddell Predictions (U = 7,500 ft/sec)

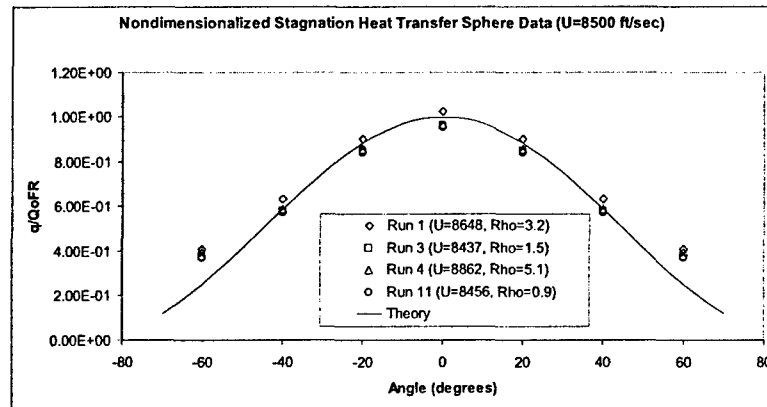


Figure 20 Comparison between Heat Transfer Measurements around a Hemispherical Noretip and Fay Riddell Predictions (U = 8,500 ft/sec)

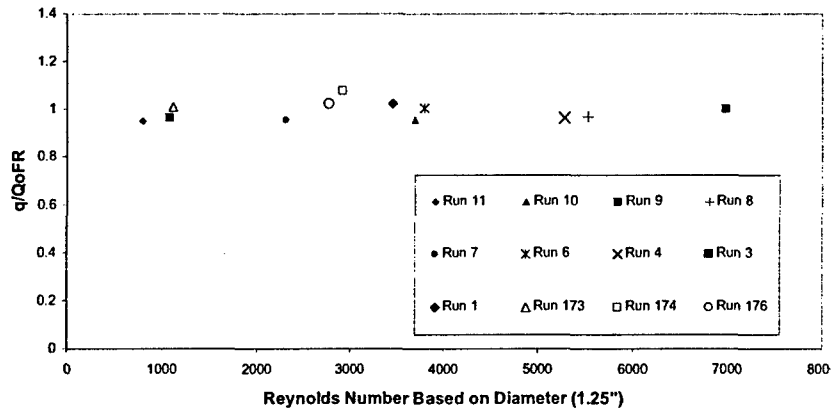


Figure 21 Variation of the Measured Stagnation Point Heating to Hemispherical Nostetip Nondimensionalized with Fay Riddell Predictions with R_{ed}

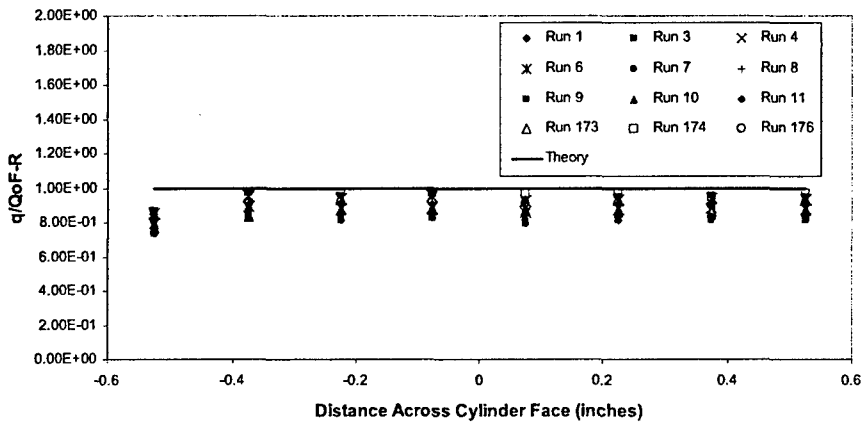


Figure 22a Stagnation Line Heating Across Cylindrical Leading Edge Reference to Predictions Using Fay Riddell Theory

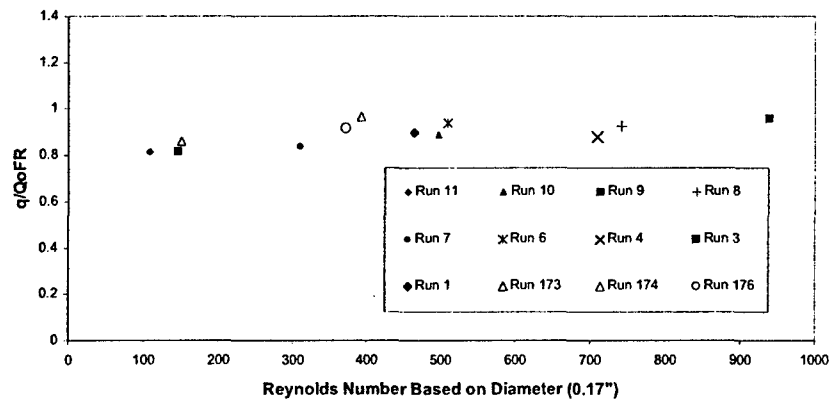


Figure 22b Variation of the Measured Stagnation Point Heating to Cylindrical Nostetip Nondimensionalized with Fay Riddell Predictions with R_{ed}

LASER DIODE MEASUREMENTS OF NONEQUILIBRIUM EFFECTS IN FACILITY AIR FLOW

Introduction

The LENS I hypersonic shock tunnel facility located in Buffalo, N.Y. is capable of producing a freestream velocity of greater than 14,000 ft/s (Ref. 6). The high enthalpy operation of the facility results in compressed and shock heated test gases than can attain a temperature of greater than 8,000°K at the end wall. At these very high temperatures the test gas undergoes dissociation. The test gas cannot recover to initial conditions due to dissociation at high temperature.

For velocities below 8,000 ft/s, the LENS I and LENS II shock tunnels produce fully duplicated conditions for a large range of flight trajectories as shown in Figure 10. At higher velocity there are small levels of dissociated products, frozen during the expansion, in the test section. Nonequilibrium chemistry models have been developed (Ref. 7), to predict the Nitric Oxide (NO) concentration in the freestream gas. At CUBRC we have constructed a continuous wave Quantum Cascade Laser (QCL) tunable-laser absorption spectrometer to measure the nitric oxide concentration, velocity and translational temperature in the freestream during the 5-10 millisecond test period of the LENS I hypersonic shock tunnel facility.

Experimental Setup and Optical Interface

The measurement of the freestream velocity in the LENS I tunnel can be obtained through absorption spectroscopy if the wavelength sensitivity of the measurement has sufficient resolution. The doppler shift technique is a robust method that depends only on the accuracy of the geometrical measurement of the projected beam path, and the accuracy of the measured wavelength shift of the absorption feature. In Figure 23 the physics of the velocity measurement is summarized.

In hypersonic test facilities the introduction of a laser beam into the flow can be complicated by boundary layer effects as the beam passes through the side walls of the facility, passing through the boundary layer of the expanding core flow. To mitigate these effects and provide the smallest possible beam steering effects for the measurement, an optical interface was designed and installed. As shown in Figure 24, the optical interface consists of two parallel plates (to the flow) with flush mounted CaF_2 windows. The flat plate arrangement is known to have a minimal beam steering effect on the laser beam, of the order of 5 microns. The flat plate probes are designed to allow for the adjustment of the plate spacing from 15 cm to 70 cm. The adjustment of the plate spacing allows the experimenter to optimize the absorption feature transmission to within the desired 80% to 10% transmission, based on the expected freestream conditions. Two inch CaF_2 windows with 30 minutes of wedge were mounted into the flat plates. The wedges were desired to minimize etalon effects from interference of the transmitted beam with secondary reflections off the surfaces of the windows. Similar windows were mounted into 16-inch optical blanks. The center spacing of the tunnel wall-mounted CaF_2 windows was 12 inches. Due to geometrical constraints and the desire to measure velocity while other probes are installed in the tunnel, the measurements had to be performed constrained to a single window blank, thus the 12-inch separation of the external tank windows. To maximize the doppler shift effect the beams were crossed and the upstream and downstream beam were measured with high speed LN_2 cooled InSb detectors with 20 ns rise time. The acquisition

system is based on 200 MHz cards providing adequate temporal resolution to measure the absorption feature line shape accurately for 1 ms scans across the nitric oxide absorption feature.

QCL Laser Spectrometer

The QCL laser spectrometer for nitric oxide measurements has been described previously; in this report we describe modifications to allow for the measurement of the freestream velocity using the Doppler shift technique (Ref. 8). The QCL spectrometer is based on a room temperature quantum cascade diode from Alpes Lasers Inc., a ZnSe aspheric lens is used to collimate the beam from the diode and project it to a turning mirror for the upstream path of the velocity measurement setup. A ZnSe wedge is used to split the beam and send a portion of the radiation to a second leg which is introduced into the tunnel at an angle downstream with the flow. The crossed beam measurement doubles the doppler effect relative to a single path perpendicular to the flow with a second beam following one of the angled paths. A schematic representation of the experimental measurement is shown in Figure 25.

In Figure 26 the schematic representation of a typical TDLAS system is presented. Note that the laser diode is driven by an increasing current, usually a ramp current. This causes the laser diode to increase in temperature and thus slightly shifts the wavelength of the laser emission. Also the intensity of the laser increases linearly with the current. Modulation of the laser current allows the experimenter to scan across the absorption feature multiple times during an experiment. Typically the scanning interval is set to between 1ms and 0.1ms. Faster scan rates imply more numerous sampling of the freestream condition, however the laser emission begins to smear and line shape analysis will not yield the translational temperature. This is a crucial issue because measurement of concentration is strongly tied to the temperature of the probed molecule.

Summary of Results

The tunable diode laser spectroscopy instrument that has been built and installed at the CUBRC hypersonic facilities has been recently modified to give freestream velocity information via the doppler shift technique. The QCL based TDLAS laser spectrometer is shown in Figure 27. The laser diode was modified to split the source beam into two paths allowing a crossed beam measurement of the absorption feature upstream and downstream relative to the flow velocity. Thus, besides yielding the concentration and temperature of the nitric oxide contained in the freestream by absorption line shape analysis, the wavelength shift of the two crossed beams yields the velocity. Eighteen experiments were performed in the LENS I tunnel for various high enthalpy conditions for freestream velocities between 2,800 m/s and 4,600 m/s. The peak shift was observed to vary from 100 MHz to 171 MHz where the peak spacing for the nitric oxide feature is 308 MHz. The peak location was obtained by fitting the doublet Doppler limited line shape to obtain the absorption feature center location. This location shift was compared between the upstream and downstream measurements as shown in Figure 28. Note that the peak separation between the upstream and down stream absorption feature is 308 MHz. The peak shift was measured to be 170 MHz which corresponds to a velocity of 4,800 m/s. In addition to velocity the translational temperature and concentration of the Nitric Oxide in the freestream was obtained from a line shape analysis of the doublet absorption feature. This is presented for run 266 as shown in Figure 29. Note the close correspondence between the data and the theoretical Voigt line shape for NO at 3.5 percent by mole-fraction for a freestream temperature of 270°K. Note the width of the double-peaked NO absorption structure. The width

of this feature is strongly dependant on the square root of the velocity according to the Doppler line shape contribution which is dominant at the freestream pressure of the flow. At the CFD computed freestream temperature for this flow, the width of the doublet would be required to be at least 20% larger than the measured width, which is clearly not supported by the measured value.

In addition to the NO absorption/velocity measurement, two H₂O transitions at 1,392 nm were measured during run 266. Analysis of the H₂O line shape yields almost the same value for the freestream temperature, 280°K as shown in Figure 30. As with the NO measurements the two lines provide a local linear wavelength calibration for the measurement. Line by line calculations based on the HITRAN 2004 data base are used to compute the H₂O line shape. As with the NO measurement a Voigt line shape is used. However, just as with the NO measurement the Doppler line shape is dominant at the flow freestream pressure. Therefore, the line shape is strongly dependent on the temperature. Line by line calculations as a function of temperature result in a temperature uncertainty for the best fit to the measured data of about 10°K.

The measurements reported here clearly establish the translational temperature of the gas in the freestream. Future measurements will be performed with species that have a pair of transitions, each transition with a sufficiently different lower state energy so that the ratio of the integrated line shape will yield the rotational temperature of the target molecules in the freestream. Also differing vibrational transitions will be probed to obtain the vibrational temperature of the target molecules in the freestream.

The studies presented here are also reported in AIAA Paper 2006-0926.

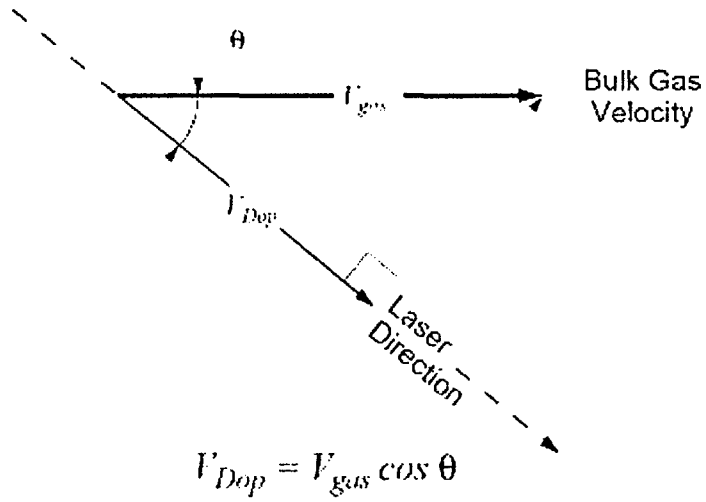


Figure 23 The Doppler Shift Velocity Technique is Based on Measuring the Wavelength of the Absorption Feature for a Laser Beam Propagating at an Angle θ Relative to the Flow

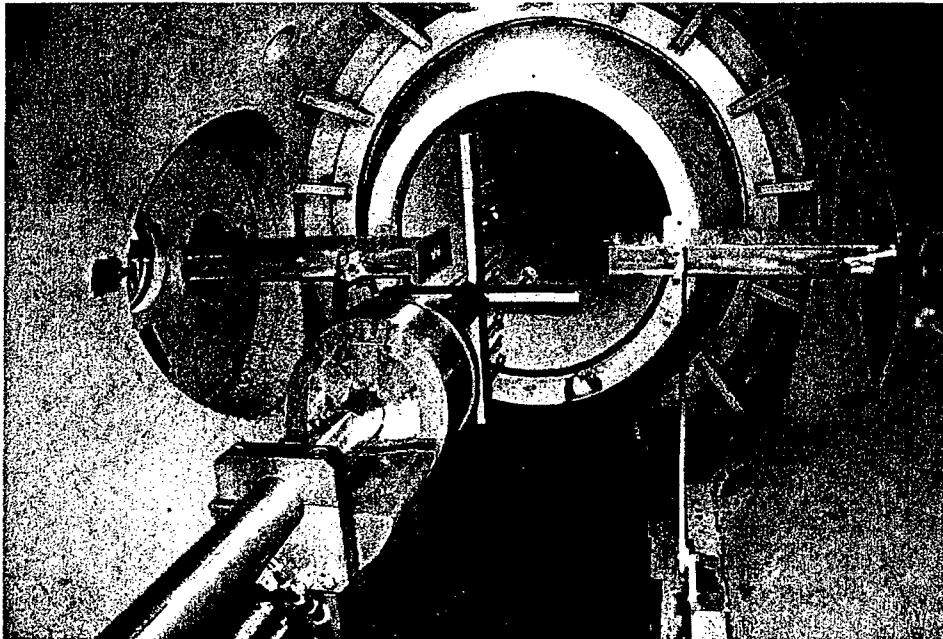


Figure 24 Flat Plate Probe Structure for the NO Freestream Velocity Measurement Installed in the LENS I Tunnel

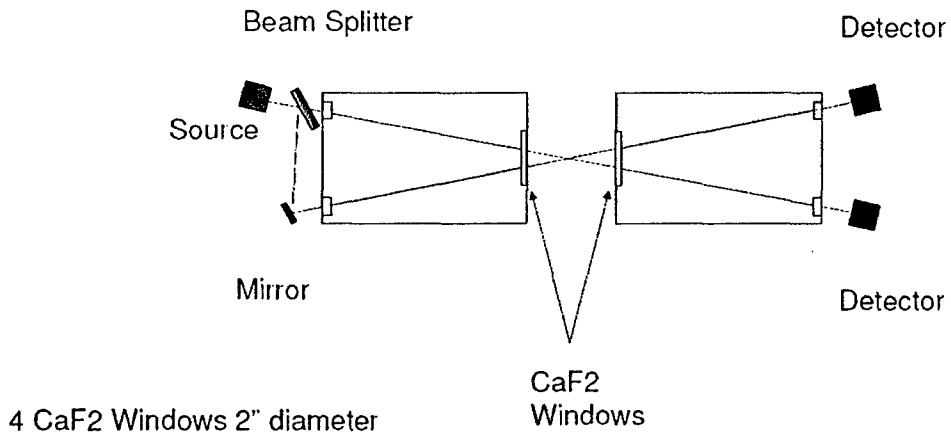


Figure 25 Schematic Representation of the Experimental Layout

Measurements of NO in Freestream and Shock Layers Employing Tunable Diode Laser Spectroscopy

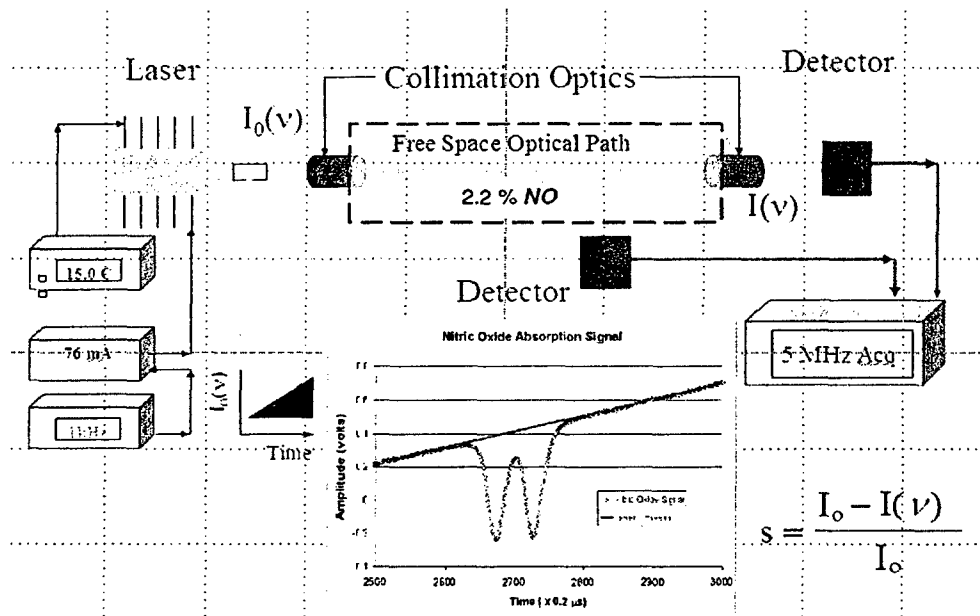
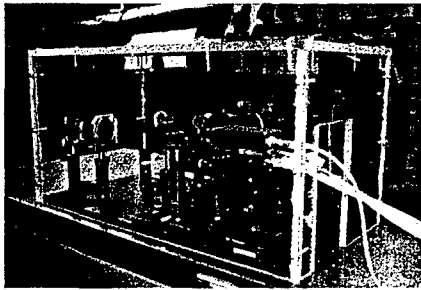
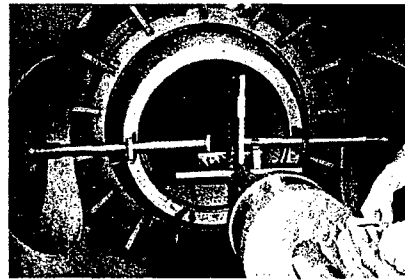


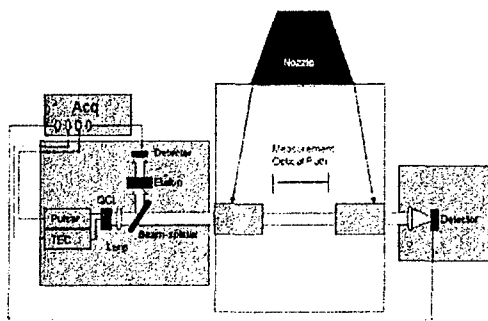
Figure 26 Schematic Representation of a TDLAS Absorption Experiment



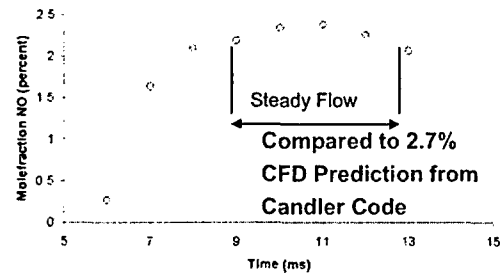
(a) Laser Diode Instrumentation



(b) NO Measurement Apparatus in LENS I



(c) Schematic Diagram of Laser Diode Setup



(d) Concentration Measurements in 48-Inch Tunnel

Figure 27 NO TDLAS Spectrometer Installed in the 48" Tunnel Facility.

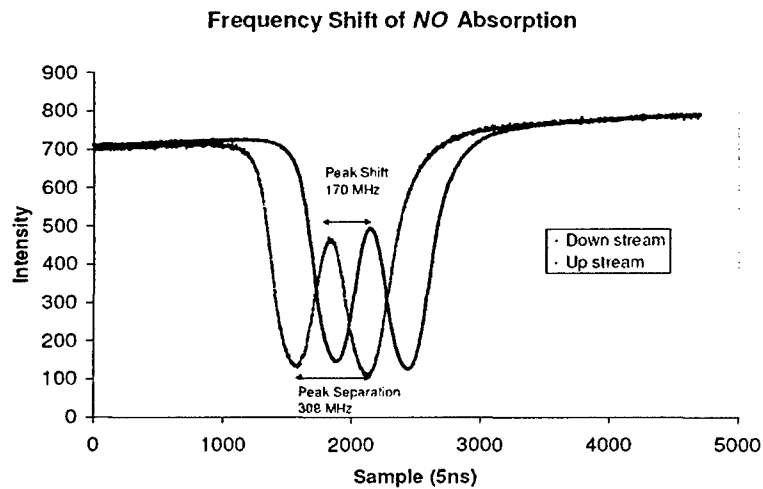


Figure 28 The Doppler Shifted Peak Location is Measured to Obtain Velocity

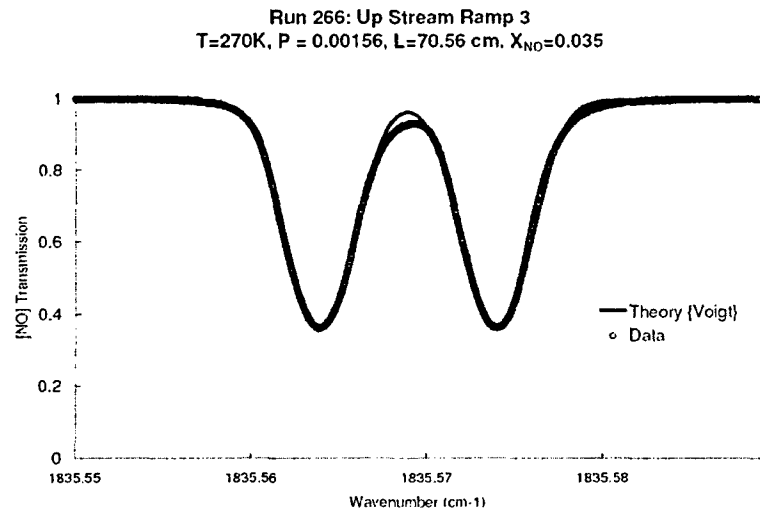


Figure 29 Best Fit to the Measured NO Line Shape for Run 266 Corresponds to a Freestream Concentration of NO of 3.5% by Molefraction for a Translational Temperature of 270°K

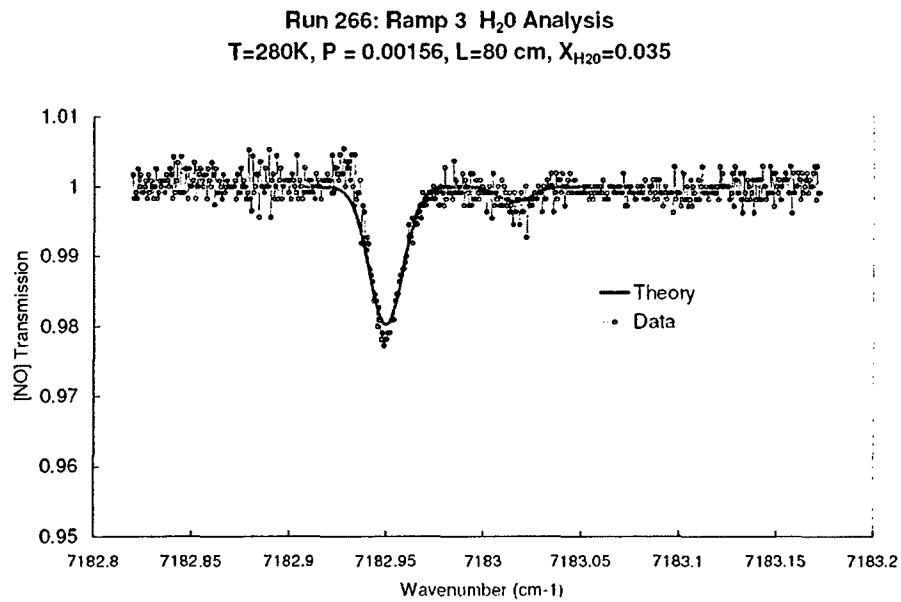


Figure 30 H₂O line Shape Measurement of the Freestream for Run 266. The Temperature of the H₂O was Determined to be 280°K

Preliminary Studies to Calibrate and Validate the LENS X Expansion Tunnel

The recently constructed LENS X facility, which is a large expansion tunnel, was developed principally to generate flows with little or no freestream dissociation at velocities between 8 kft/sec to 15 kft/sec. The tunnel also has the potential to provide testing at velocities over 7 km/sec and produce effective reservoir pressure conditions of well over 100,000 psi. The addition of this new facility also provides us with the capabilities to conduct "free jet" scramjet engine tests up to Mach 15. The viability of expansion tunnels to generate high-quality flows for large-scale hypervelocity testing has been the subject of significant debate since its conception because of questions associated with dynamic instabilities that can arise at the interfaces and shock fronts between the gases in the driver, driven, expansion and nozzle sections of the tunnel as well as the viscous interaction phenomena associated with thick boundary layers generated on the walls of the expansion section of the tunnel (see Ref. 4). In theory, these effects should be less deleterious in a large facility like LENS X; however, the major concerns expressed over the years on the performance of the expansion tunnel led us to install a significant amount of surface and flowfield instrumentation throughout the new tunnel similar to that employed in LENS I.

The LENS X is assembled with major components from the LENS II facility together with new diaphragm stations and tube components. This tunnel shares compressors, vacuum pumps, and the data system with the other LENS tunnels. A schematic diagram of the LENS facility is shown together with a schematic of the LENS X facility in Figure 31. The LENS X facility is over 200 ft long and is joined to the test section through a modified LENS II nozzle. The tunnel has an electrically heated driver section in which hydrogen, helium, and nitrogen can be employed as driver gases. The flow is initiated through the tunnel using a double diaphragm valve which connects the driver and driven section of the tunnel. The gases in the driven and expansion sections of the tunnel are separated by a single thin plastic diaphragm. A diaphragm can also be installed to isolate the gases in the expansion tube from those in the test section, however in the present studies, we ran with these two components connected at the same low pressure. A wave diagram illustrating the operation of the LENS X facility is shown in Figure 32 together with a pitot pressure trace taken from probes positioned at the end of the expansion tube. For the 15 kft/sec conditions, we obtained test times of close to 2 msec in Region 5 at the end of the expansion tube. A wave diagram for this condition generated using the method of characteristics employed in the Kasimir code is shown in Figure 33. Shown in Figure 34 is the prediction of the static pressure on the wall at the end of expansion tube obtained from the Kasimir code. The actual measurement of static pressure on the tunnel wall for these conditions is shown in Figure 35a and is in close agreement with the inviscid flow prediction in Figure 35b. Measurements made with a pitot pressure rake positioned at the end of the expansion tube are shown in Figure 36a and compared with the predicted values in Figure 36b (Ref. 9).

The remarkably good agreement between inviscid flow predictions and the measured wall and pitot pressures in LENS X suggest that the tunnel performs extremely well and the instabilities that could occur at the interfaces do not significantly degrade tunnel performance. Flowfield surveys using pitot pressure, total heat transfer and static pressure probes were obtained at the exit plane of the nozzle for the two major test conditions selected for the double cone studies. We also obtained interferograms of the flow over hemispheres and cylinders for comparison with numerical computation. Figure 37 shows an interferogram obtained in air and a numerical simulation of this flow obtained by Candler (Ref. 9) can be seen to be in close agreement. *The results discussed here were discussed in AIAA Paper 2005-4694.*

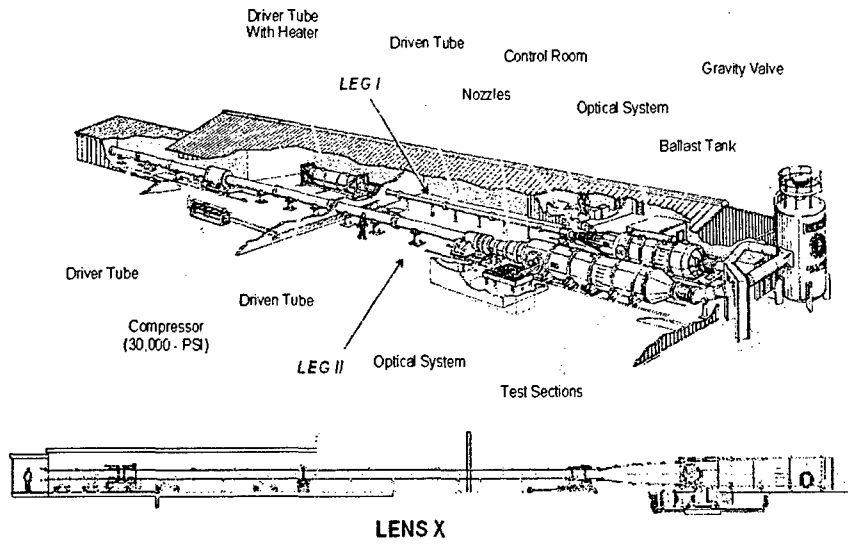


Figure 31 Layout of LENS I, II and X Supersonic and Hypersonic Facilities

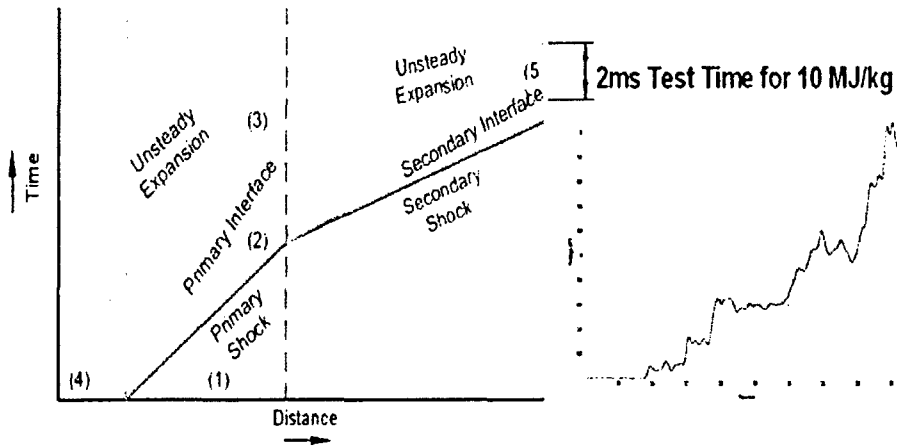
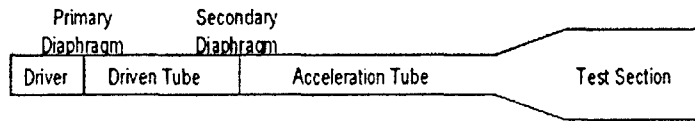


Figure 32 Wave Diagram of the Operation of the LENS X Expansion Tunnel

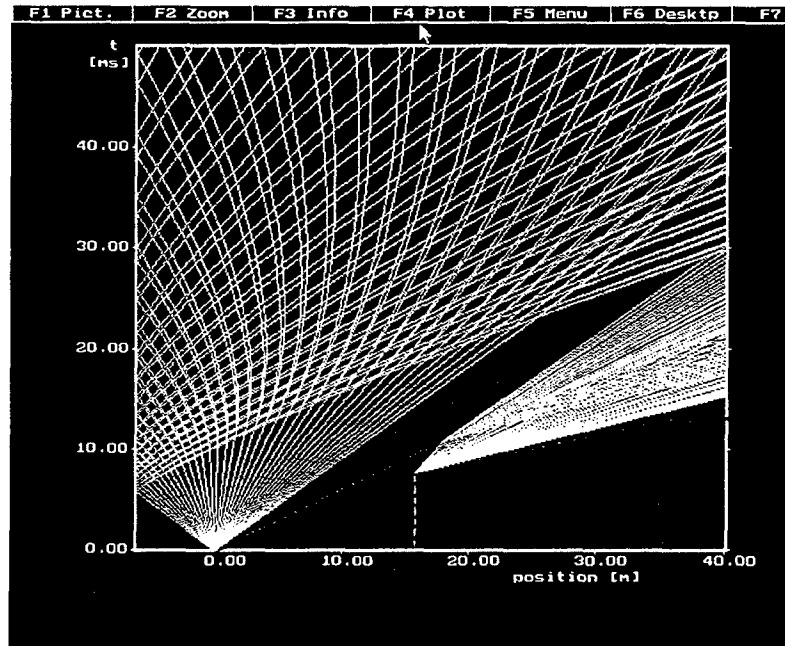


Figure 33 Method of Characteristic Calculations using Kasimir Code to Evaluate Test Time and Test Conditions in LENS X

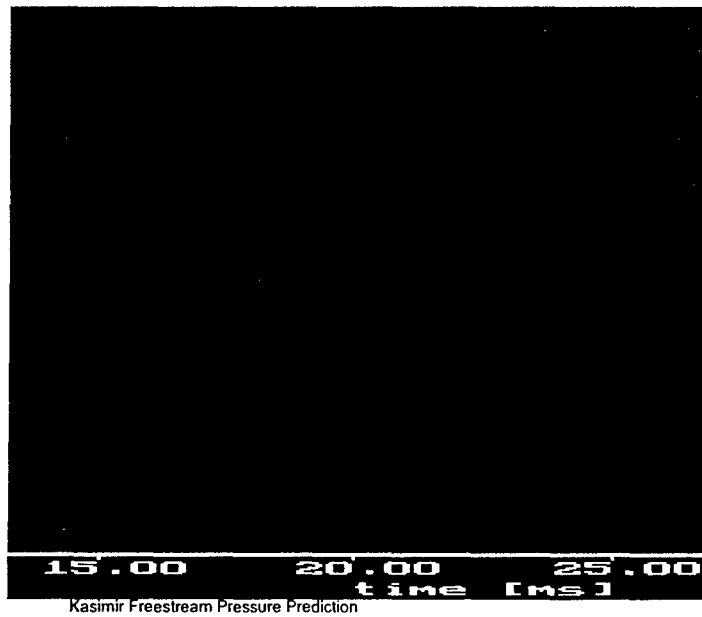


Figure 34 Freestream Static Pressure Prediction from the Kasimir Code

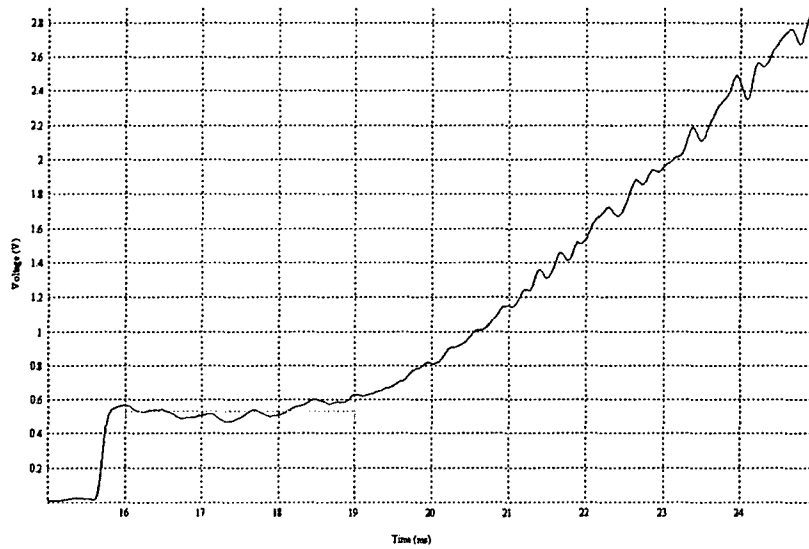


Figure 35(a) LENS X Static Pressure Measurements at End of Expansion Section Compared with Prediction from the Kasimir Code in Figure 34

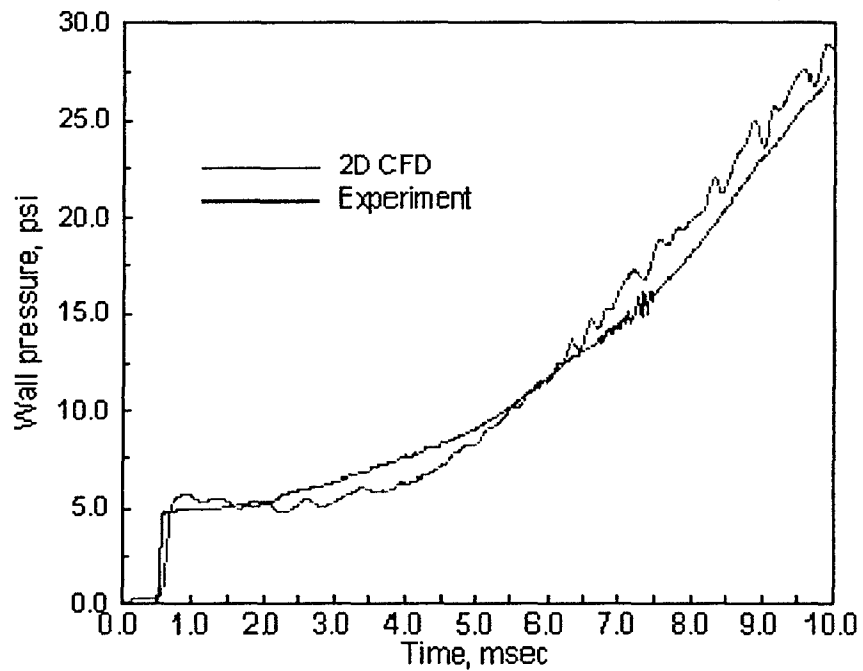


Figure 35(b) LENS X Static Pressure Measurements at End of Expansion Section Compared with Navier-Stokes Predictions (Ref. 9)

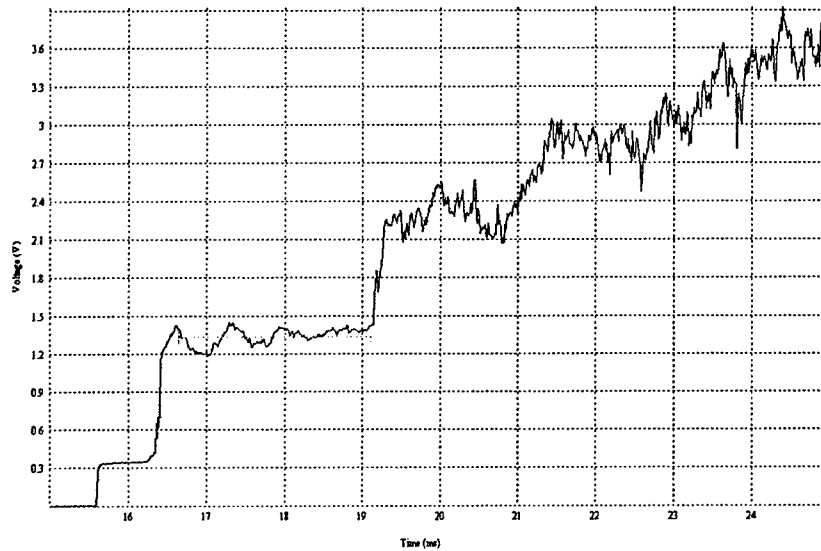


Figure 36(a) LENS X Pitot Pressure Measurement at End of Expansion Section

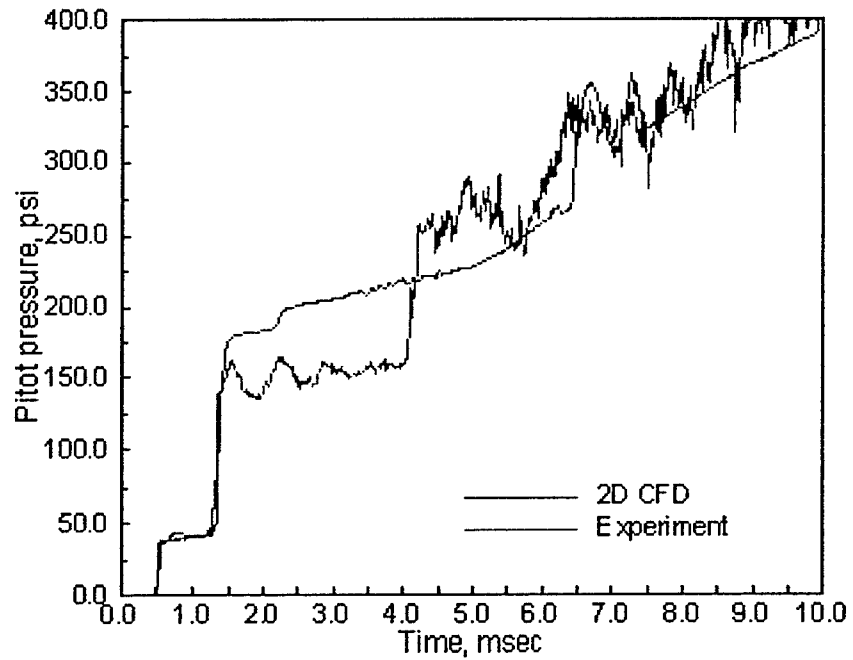


Figure 36(b) LENS X Pitot Pressure Measurement at End of Expansion Section Compared with Navier-Stokes Predictions (Ref. 9)

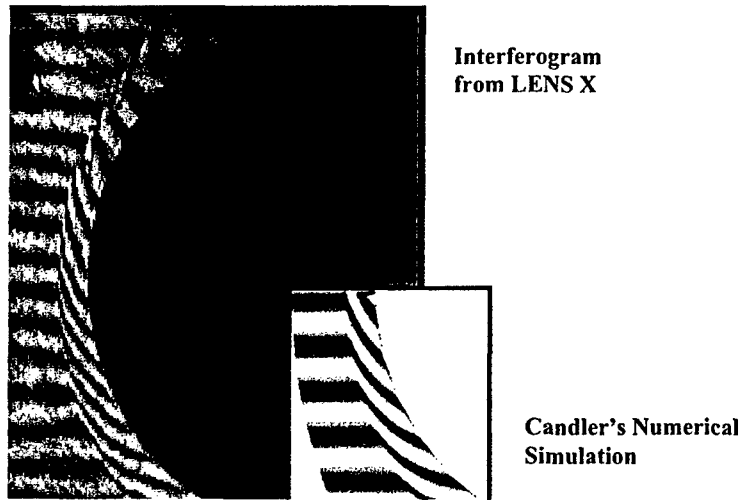


Figure 37 Comparison between Interferograms Obtained in Experiment and Prediction on Spherical Nosetip (Ref. 9)

MEASUREMENTS IN LOW DENSITY FLOWS ON THE HOLLOW CYLINDER/ FLARE AND DOUBLE CONE CONFIGURATION AND COMPARISONS WITH IMPROVED NAVIER-STOKES AND DSMC PREDICTION METHODS

Introduction

During the course of this program, measurements were conducted with the hollow cylinder/flare and double cone models in the LENS I and 48-inch tunnels, together with new computations using recently improved DSMC techniques and the Navier-Stokes methods. In these studies we employed the hollow cylinder/flare configuration shown in Figure 38 which was extensively instrumented with thin-film platinum heat transfer gages and contains new flush mounted pressure instrumentation specifically designed to accurately measure low pressures on the cylinder in low density flows. The double cone model shown in Figure 39 contains high-frequency piezoelectric pressure gages and platinum thin film heat transfer gages. Back-to-back measurements were made with both the hollow cylinder/flare and double cone model in the LENS I and 48-inch tunnels to compare and validate the measurements in the two different facilities, in a number of cases with two different instrumentation sets. As part of the tunnel and instrumentation validation program, we also compared the measurements obtained on the aforementioned double cone configuration with those obtained on a second double cone model containing thermocouple heat transfer gages which was fabricated specifically for the real gas studies.

Studies with the Hollow Cylinder/Flare Configuration

The most recent studies with the hollow cylinder/flare configuration were conducted in the lower density flow regime for the specific purpose of evaluating the new numerical procedures employed in the contemporary DSMC prediction methods, and the formulations that account for surface slip in the Navier-Stokes computations. As discussed above, measurements were made in both the LENS I facility and the 48-inch shock tunnel specifically to evaluate the accuracy of the combined facility instrumentation, data reduction procedures, and flow conditions.

Shown in Figure 40 are comparisons between the pressure and heat transfer measurements over the hollow cylinder/flare configuration made in the 48-inch shock tunnel and the LENS I facility. These sets of measurements are in good agreement both on the cylinder and flare portions of the model and demonstrate that combined facility/ instrumentation accuracy is better than 5 percent. The calculations obtained by Candler (Ref. 10) for the test case shown in Figure 41 do not appear to be significantly influenced by surface slip, although including surface slip appears to decrease the length of the interaction region and lower the heat transfer rate slightly below the values measured in experiments. The DSMC calculations by Markelov (Ref. 11) shown in Figure 42 are in good agreement with the pressure data both on the hollow cylinder and on the flare but also slightly underpredict the length of the interaction region and the heating on the flare. In Figure 43 we show calculations by Boyd (Ref. 12), which were updated values of those communicated to us earlier. The new calculations are in better agreement with both the pressure and heat transfer measurements, basically mirroring those obtained by Markelov, although the computations do not extend to the full length of the flare. It is noted that this flow remains attached and the past DSMC technique did not compare as well with well-separated flows over this configuration. Thus further calculations using the DSMC method with improved numerics should be pursued to calculate higher density well separated flows over the hollow cylinder/flare model.

Studies with the Double Cone Configuration

Measurements were made with both the original 25°/55° double cone model and a new 25°/55° double cone model equipped with more robust pressure and heat transfer instrumentation designed for use in the LENS I and LENS X facilities in high enthalpy flows. Under high enthalpy conditions, thin film heat transfer instrumentation can be damaged in the LENS X facility. Comparisons between the measurements in the LENS I and 48-inch tunnel are shown in Figure 44 at similar test conditions. There is generally good agreement between the two sets of measurements, with a small difference in the reattachment compression region resulting possibly from small differences in the test conditions at which the individual studies were conducted.

At the lower density nitrogen flow conditions selected for these comparisons, Candler's Navier-Stokes solutions incorporating surface slip accurately predict the pressure and heat transfer distribution throughout the interaction region as shown in Figure 45. However, although incorporating slip effects improves agreement with heat transfer rate on the first cone, they lower the predictions to below the measured values on the flare. The calculations by Moss shown in Figure 46 using the newly improved Bird prediction methodology not only are capable of efficiently calculating the flow over the double cone configuration, they are in excellent agreement with the experimental data for this well-separated flow induced by complex regions of shock/boundary layer and shock/shock interaction. Moss' calculations (Ref. 13) are all the more impressive because they did not require extensive use of large scale parallel computing capabilities. A similar set of calculations for the double cone configuration obtained by Markelov, shown in Figure 47, are also in good agreement with the measurements, although this set of calculations slightly underpredict the heat transfer rate both upstream and downstream of the interaction region. Both sets of DSMC calculations and the Navier-Stokes solutions accurately predict the length of the separated and shock/shock interaction region. This good agreement again suggests that the focus in our code validation activities should be turned to more complex flows involving first real gas chemistry and later turbulent flows.

The results are also presented in AIAA Paper 2004-0917

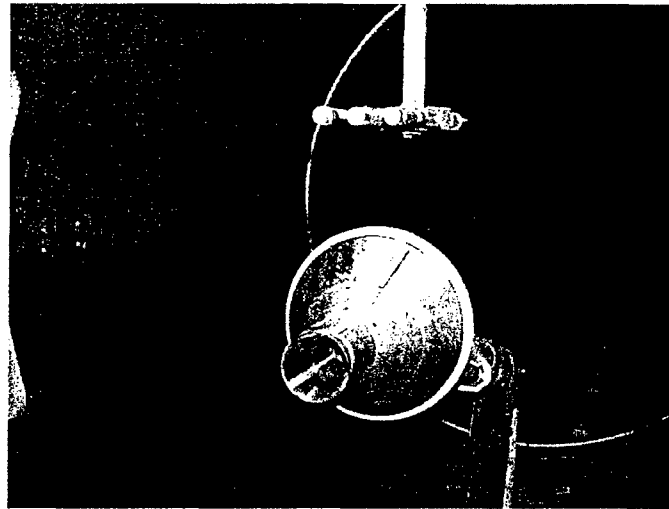


Figure 38 Hollow Cylinder/Flare Model Used in Studies

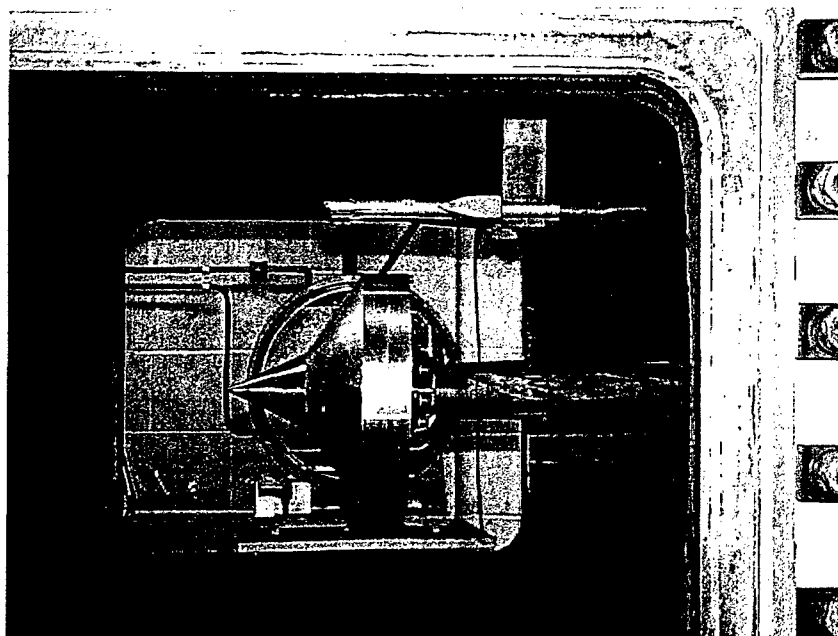


Figure 39 Double Cone Configuration Used in Studies in 48-Inch Shock Tunnel

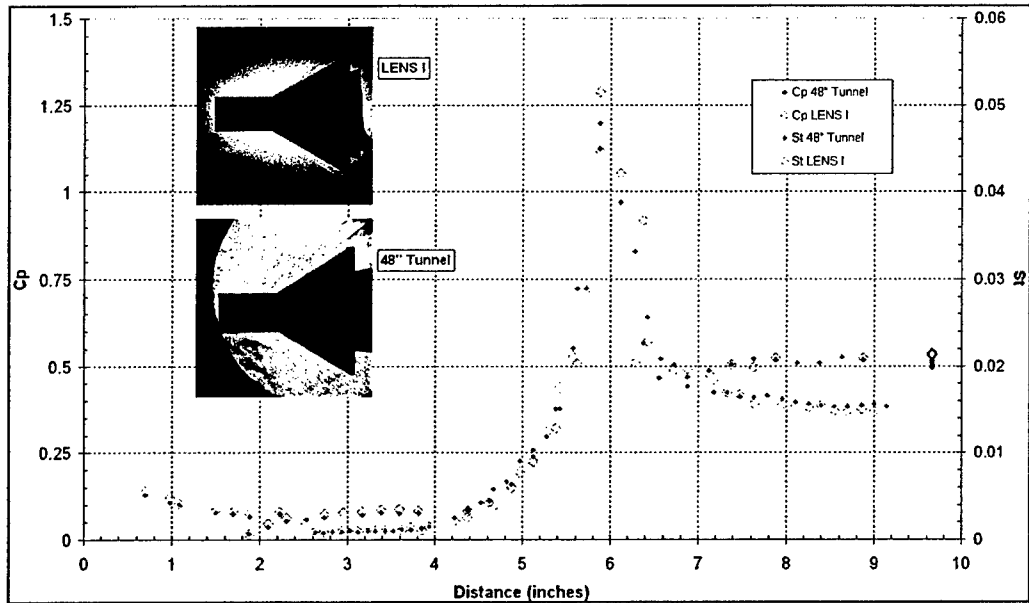


Figure 40 Comparisons between Pressure and Heat Transfer Measurements in 48-Inch and LENS I tunnels

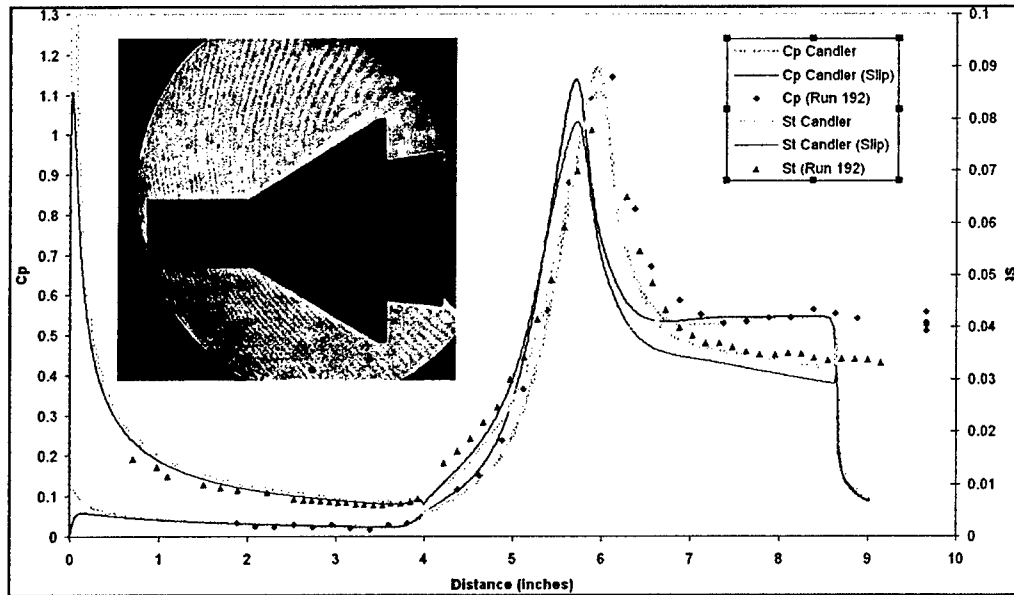


Figure 41 Heat Transfer and Pressure Measurements compared with Navier-Stokes Calculations by Candler

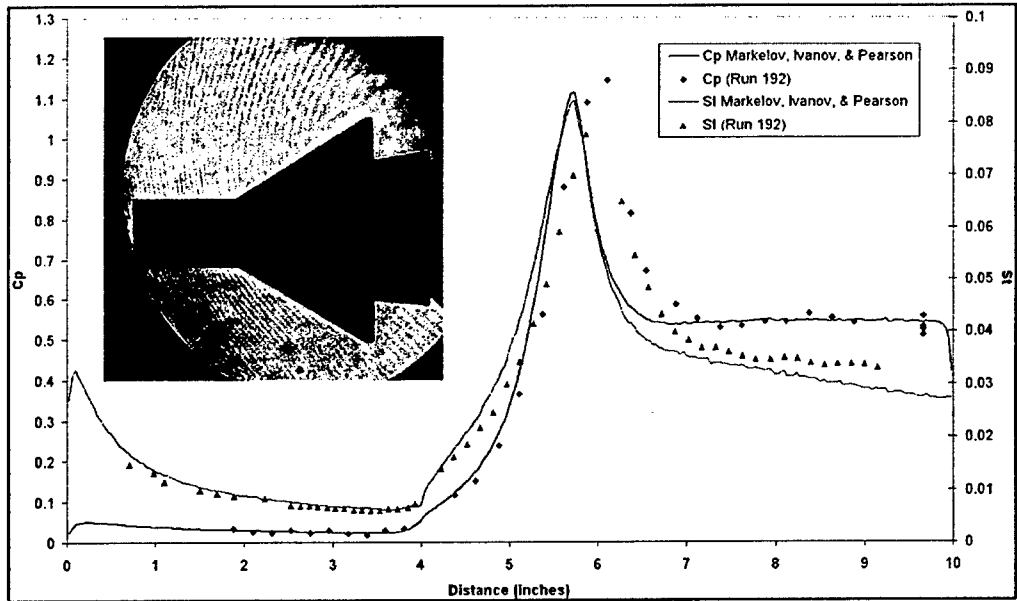


Figure 42 Heat Transfer and Pressure Measurements Compared to DSMC Calculations by Markelov

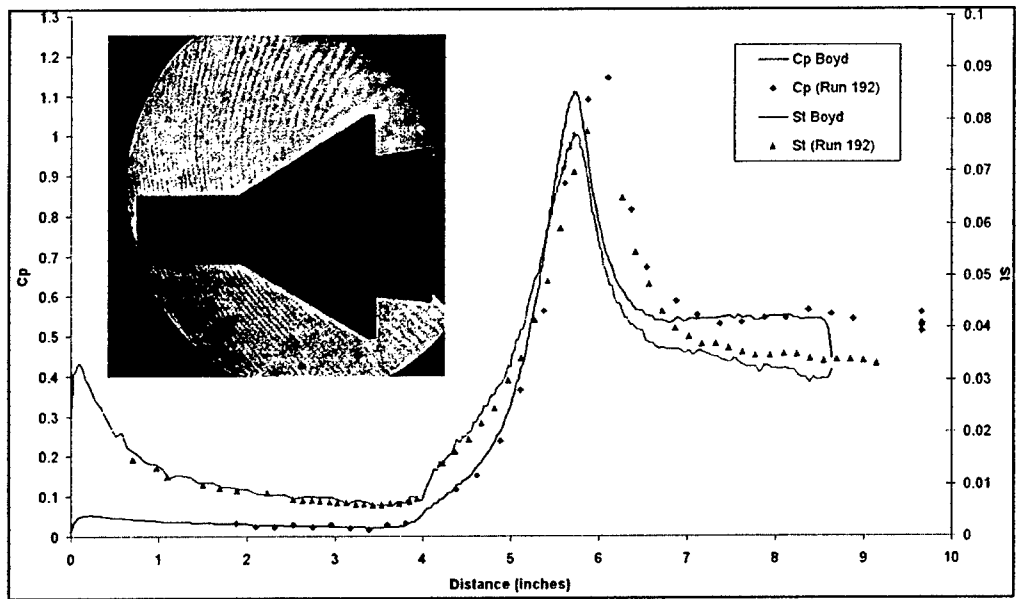


Figure 43 Heat Transfer and Pressure Measurements Compared to DSMC Calculations by Boyd

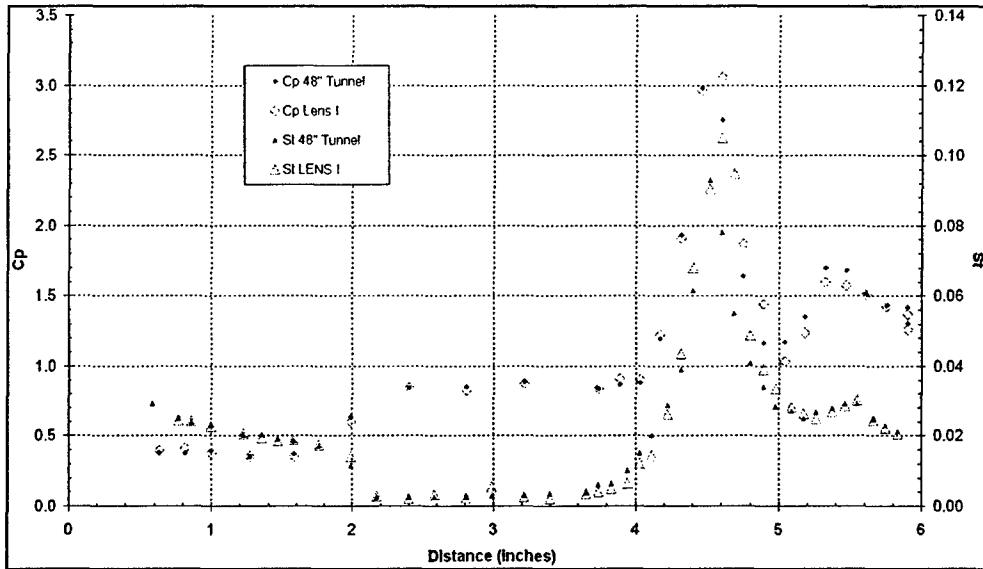


Figure 44 Pressure and Heat Transfer Measurements on Double Cone Configuration in 48-Inch Tunnel and LENS I

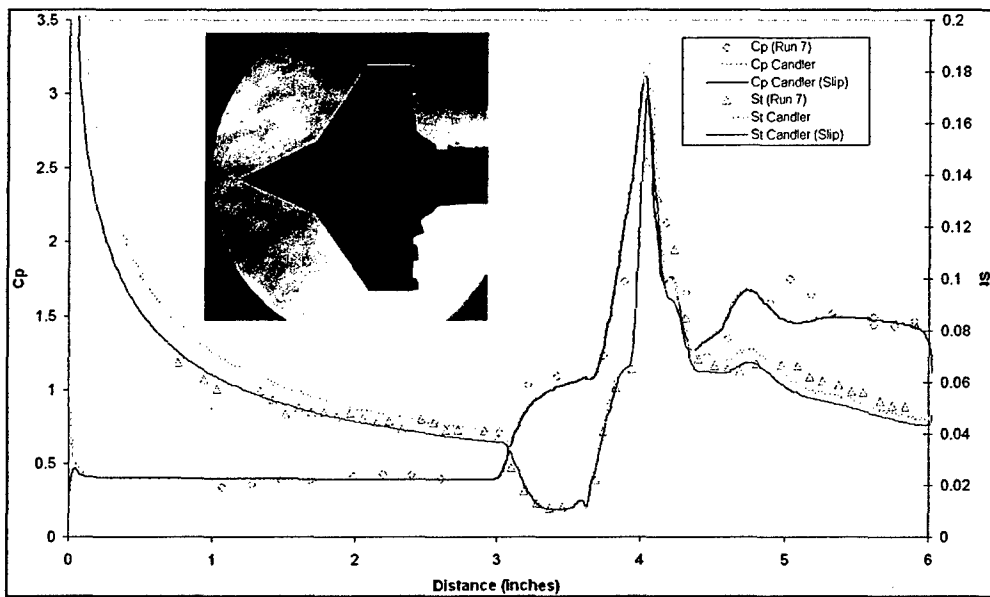


Figure 45 Comparison between Heat Transfer and Pressure Measurements and Navier-Stokes Calculations incorporating Surface Slip by Candler

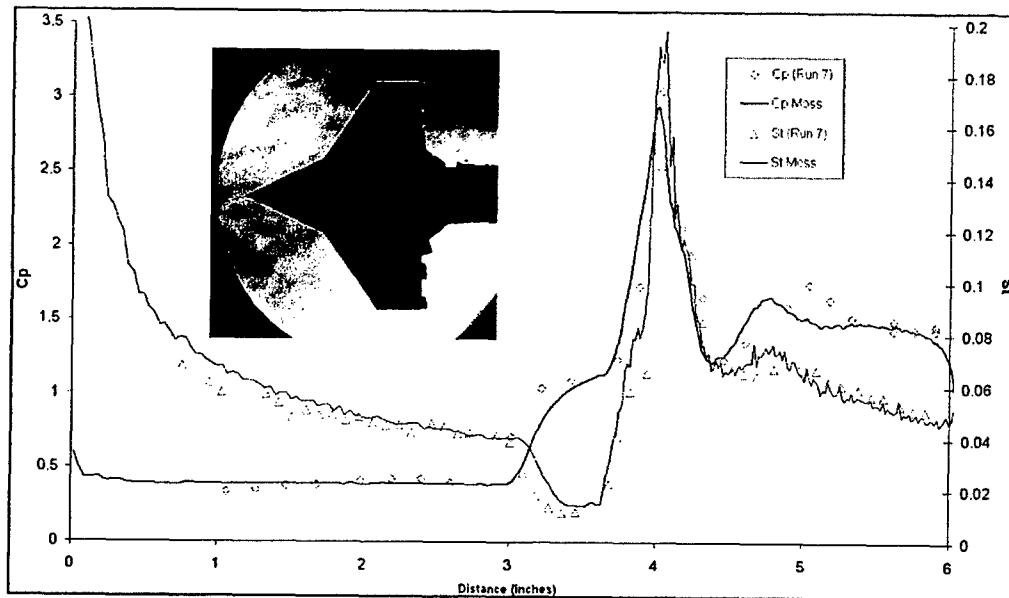


Figure 46 Heat Transfer and Pressure Measurements Compared to DSMC Calculations by Moss

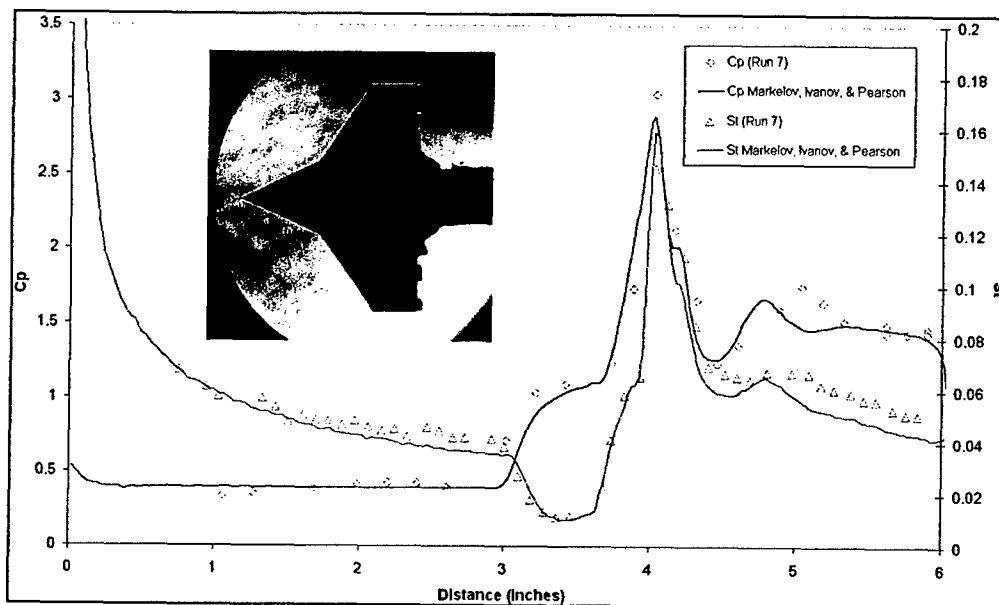


Figure 47 Heat Transfer and Pressure Measurements Compared to DSMC Calculations by Markelov

STUDIES OF REAL GAS EFFECTS IN HIGH ENTHALPY FLOWS FOR FACILITY AND CODE VALIDATION

Introduction

Following the extensive series of flow calibration studies in the LENS facilities (see Figure 48) discussed in the previous section, we embarked on a series of studies first with simple nose shapes, a cylinder, hemisphere, blunt ended cylinder and a spherically blunted 70° cone to provide measurements of the shock shape and the distributions of heat transfer and pressure to compare with Navier-Stokes calculations. These studies were conducted in nitrogen, air and CO_2 in both high and low enthalpy flows to examine real gas effects and shock shape and shock standoff distance as well as providing information with which to begin the examination of surface catalysis on the distribution of heating around the nose shape. The selection of CO_2 as a test gas was done on the basis of both interest in planetary entry as well as the more complex real gas chemistry which could provide important information on the validity of the models of vibrational dissociation and coupling and the transitions between electronic states excited in the high enthalpy flows. The wind tunnel calibrations with CO_2 demonstrated good flow uniformity at the exit plane of the nozzle on par with that of both nitrogen and air flows. The double cone configuration and then the shuttle configuration were used in the major part of this program to explore real gas effects on regions of shock wave/boundary layer interaction both in air and nitrogen flows. The studies with the shuttle configuration were devised to provide the first definitive experimental measurements to attempt to explain the so-called trim anomaly where the flap measurements of the pitching moment of the shuttle differed significantly from those predicted on the basis of ground test data.

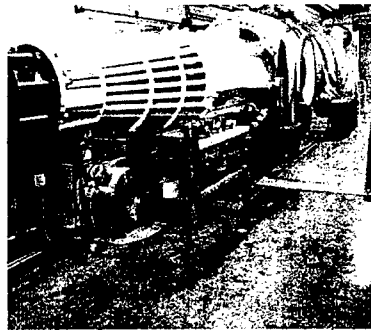
Real Gas Effects in Hypervelocity N_2 , Air and CO_2 Flows on Simple Nose Shapes

To systematically evaluate real gas effects, we have performed a series of studies in air, nitrogen and CO_2 on blunt nosetip configurations in parallel with measurements using laser diode techniques to evaluate the properties, in particular the levels of NO , in the freestream. Both these studies are supported with calculations with the DPLR code (Ref. 14). The studies in air were conducted at 5 MJ/kg and 10 MJ/kg with a cylindrical model equipped with high-frequency pressure and heat transfer instrumentation and with high speed Schlieren to visualize the characteristics of the shock layer. Figure 49 shows calculations for real and perfect gas boundary conditions demonstrating the significant real gas effects on the standoff distance and its variation with flow total enthalpy. These calculations were validated by measurements in the LENS I facility of the shock standoff distance ahead of a cylinder for total enthalpy levels of 5 MJ/kg and 10 MJ/kg as shown in Figure 50. Also in Figure 50 we show comparisons between predictions and measurements of pressure around the cylinder at the two enthalpies and the prediction of heating levels for non- and fully catalytic surface recombination for the wall boundary condition. It is clear that while the pressure is accurately predicted for these two enthalpy levels, the heating levels to the catalytic model surface at the higher enthalpy is not well predicted, which again suggests problems with describing and predicting the flow chemistry for high enthalpy air flows.

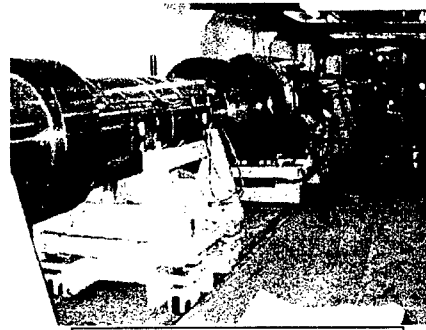
During this segment of the program, measurements were made in air and nitrogen at a range of freestream enthalpies from 2 to 14 MJ/kg over a series of blunt nose tip configurations including the 2D cylinder, a hemisphere, a flat-ended cylinder, and a 70° cone shape typical of a planetary probe configuration. Comparisons between predicted and measured shock shape over these blunt configurations in a low enthalpy (2 MJ/kg) CO_2 flow are shown in Figure 51. At

these low enthalpies, we obtain good agreement between measured and predicted shock shape. However, at higher enthalpy conditions (3, 5 and 10 MJ/kg), we increasingly see a discrepancy between measured and predicted shock shapes. A major objective of the CO₂ studies has also been to measure levels of heating as the enhancement in heating associated with the catalytic heating at the wall. These studies have been conducted in the AFOSR program in conjunction with transition studies for NASA (Ref. 15) employing an MSL configuration. Measurements of the heat transfer and pressure distribution over 1-ft and 2-ft diameter models of the MSL have been made with high frequency pressure gages and three different types of heat transfer instrumentation to evaluate the relative effects of stainless steel, platinum and silver on catalytic heating. The experimental studies have been accompanied by detailed computations of the flow in the facility and over the models using the DPLR Code as described by MacLean (Ref. 16). The heat transfer measurements made from the various gages in these studies were in excellent agreement and we have consistently observed that these measurements are in best agreement with theoretical predictions when a supercatalytic boundary is employed in the numerical calculation. Although as shown in Figure 52 and observed in our earlier studies with air, agreement between theory and measurement is closer at the lower enthalpy conditions.

The results of this study are also presented in AIAA Paper 2005-4693 and AIAA Paper 2006-0182.

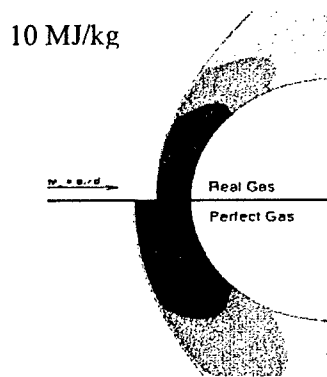


LENS I
 Velocity Range (ft/sec)
 3,000 – 15,000
 Altitude (kft)
 25 - 300
 Mach Numbers
 8.0 - 18.0
 Reynolds Numbers (1/ft)
 1.0E4 - 1.0E8
 Test Time (ms)
 up to 25
 Nozzles
 Mach 8 – 10 (48" Exit)
 Mach 10 – 18 (48" Exit)

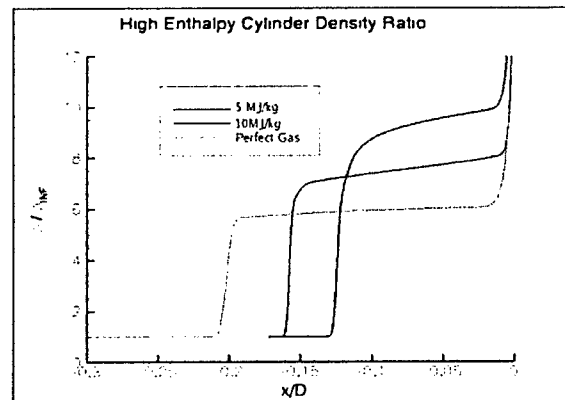


LENS X
 Velocity Range (ft/sec)
 14,000 – 22,000
 Altitude (kft)
 120 - 250
 Mach Numbers
 14.0 - 22.0
 Reynolds Numbers (1/ft)
 1.0E3 - 1.0E6
 Test Time (ms)
 up to 4
 Nozzles
 Mach 14 – 22 (60" Exit)

Figure 48 The LENS Hypervelocity Facility Employed in Studies of Real Gas Effects

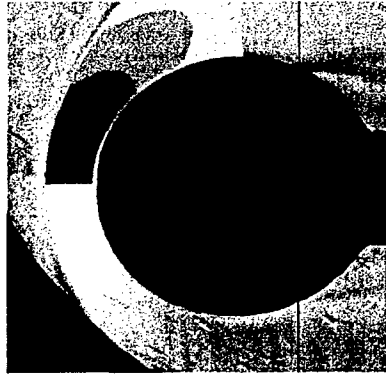


(a) Prediction of Shock Layer Characteristics for Perfect and Real Gas Flows over Cylinder

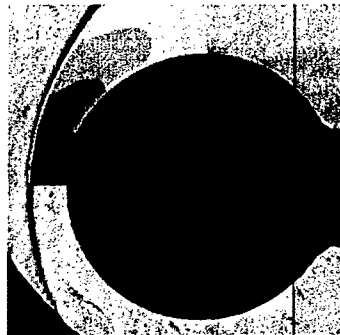
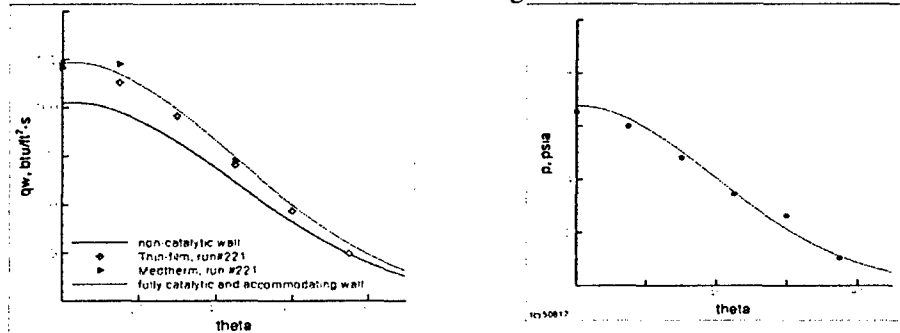


(b) Variation of Shock Position with Flow Enthalpy

Figure 49 Real Gas Effects on Shock Standoff and Shock Layer Characteristics



5 MJ/kg



10 MJ/kg

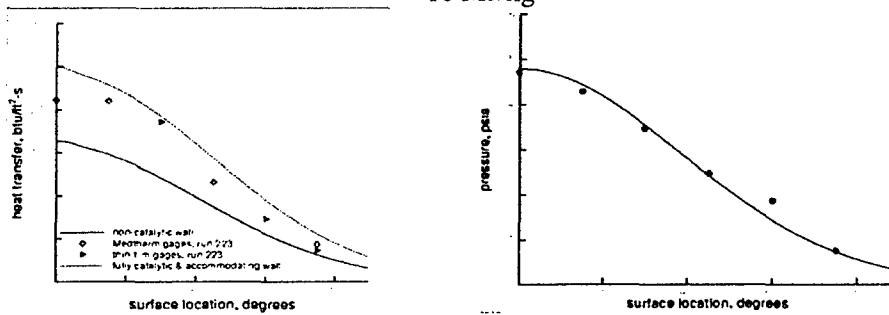


Figure 50 Comparison between Predicted Shock Layer and Surface Characteristics for Real Gas Air Flows at Total Enthalpies of 5 and 10 MJ/kg

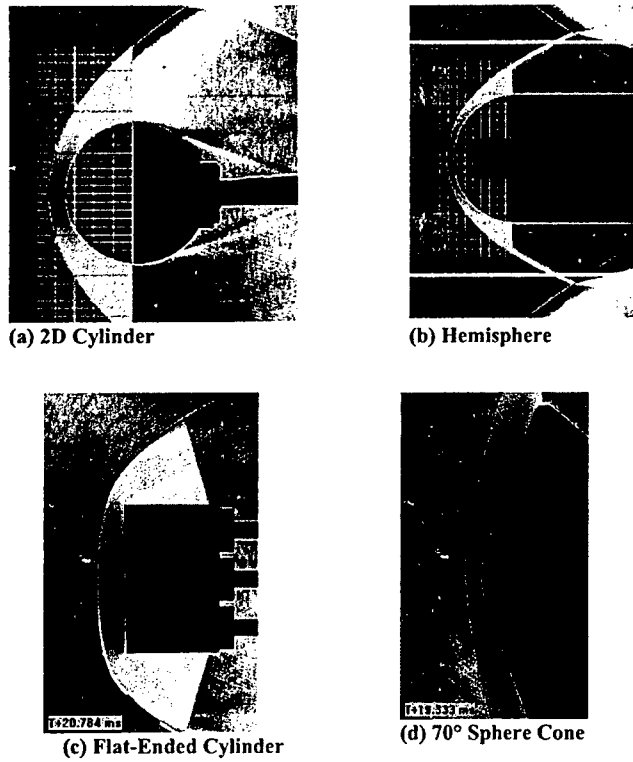


Figure 51 Comparison between Prediction and Measurement of Shock Shapes over Blunt Bodies in CO₂ for 2 MJ/kg Flow Conditions

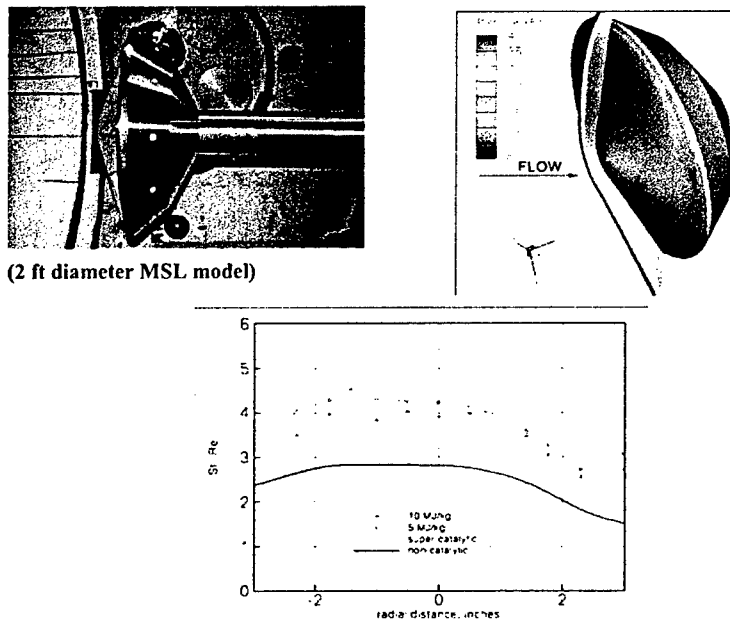


Figure 52 Measurements of Catalytic Wall Heating on Planetary Probe Configuration

MEASUREMENTS OF REAL GAS EFFECTS ON THE DOUBLE CONE CONFIGURATION IN THE LENS I SHOCK TUNNEL AND LENS X EXPANSION TUNNEL

Introduction

The double cone configuration was selected for studies of combined viscous/inviscid interaction and real gas effects specifically because earlier calculations by Candler had suggested that the size and characteristics of the separated and shock/shock interaction regions would be sensitive to real gas effects. The test conditions selected for these studies were chosen to obtain the highest possible density to maximize nonequilibrium effects over the model, while generating Reynolds numbers at which the boundary layer would remain laminar on the second flare downstream of the interaction region. We also selected the Reynolds number for the test case to achieve a well-defined separated region with well-defined attached flows both upstream and downstream of the interaction region.

Studies of Real Gas Effects on Regions of Separated Flow and Shock/Shock Interaction on the Double Cone Configuration in LENS I

These experimental studies were conducted in the LENS I facility in nitrogen and air flows at velocities of 10 kft/s and 14 kft/s at the same unit Reynolds number of $1 \times 10^5/\text{ft}$. Figure 53 shows a Schlieren photograph of the flow and distributions of heat transfer and pressure obtained in nitrogen flow over the model at a freestream velocity of 10 kft/s. This set of measurements adequately defines the length of the separated region and the peak heating and pressure in the reattachment/ shock interaction process occurring on the second cone. Also the pressure on the second cone returns to a level close to a Newtonian value producing a well-defined downstream boundary condition. Similar measurements in air at close to the same velocity and Reynolds number are shown in Figure 54. We obtained well-defined regions upstream and downstream of the separated region, and the distribution in the peak pressure and heating distribution on the second cone are well defined by the measurements. Comparing the measurements made in air and nitrogen in Figure 55, we see that both the nondimensionalized heat transfer and pressure distributions are almost identical, indicating insignificant real gas effects on the length of the interaction region and the peak heating. In the air freestream generated at this condition, the mole fraction of the NO concentration is approximately 5 percent, and clearly this does not significantly influence the characteristics of the interaction region.

At this juncture in the program we chose not to pursue an examination of nosetip bluntness and unit Reynolds number effects at the lower velocity condition to place the major emphasis on the examination of real gas effects at the higher velocity condition. Again, measurements were made with air and nitrogen, for Reynolds numbers low enough to maintain a laminar boundary layer on the second cone. Figure 56 shows the distribution of heat transfer and pressure and a Schlieren photograph of the flow with nitrogen as a test gas. The measurements indicate well-defined regions of attached flow upstream and downstream of the well-separated interaction region and sufficient measurements in the pressure and peak heating region to accurately define the distributions. A similar set of measurements for the air flow are shown in Figure 57. Again, the flow is well defined; however in this case the lengths of the separated region and the reattachment compression region are slightly shorter. The decrease in the length of the interaction region is shown more definitively in Figure 58 where the two sets of pressure measurements are plotted together.

To validate that boundary layer transition did not influence these results, we repeated the measurements at a higher Reynolds number to examine the variation in the heating levels downstream of the reattachment region with unit Reynolds number. As shown in Figures 59 and 60, we do not see a significant change in the Stanton number downstream of the interaction. Plotting the Stanton numbers from the measurements at the two Reynolds numbers in Figure 61, it can be seen that the Stanton number downstream of reattachment decreases with increasing Reynolds number as would be predicted for fully laminar flow. Therefore, it is concluded that the viscous flow remains laminar in the interaction regions developed over the models in all the experiments.

It is concluded from this set of experiments that real gas effects can decrease the length of the separated region and significantly change the structure of the reattachment/shock/shock region over the double cone. It remains to be determined whether the levels of freestream non-equilibrium can influence this result. For this reason, experiments were initiated in the LENS X facility where it is possible to generate freestreams of equal velocity in the absence of significant oxygen dissociation.

The results of this section are also presented in AIAA Paper 2006-0125.

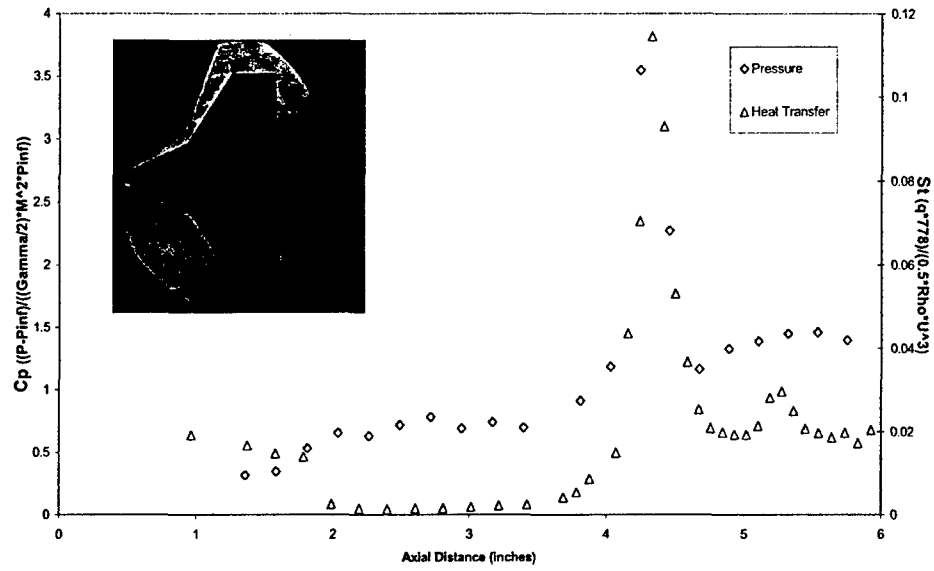


Figure 53 Schlieren Photograph and Measurement of Heat Transfer and Pressure for a 10 kft/s Nitrogen Flow

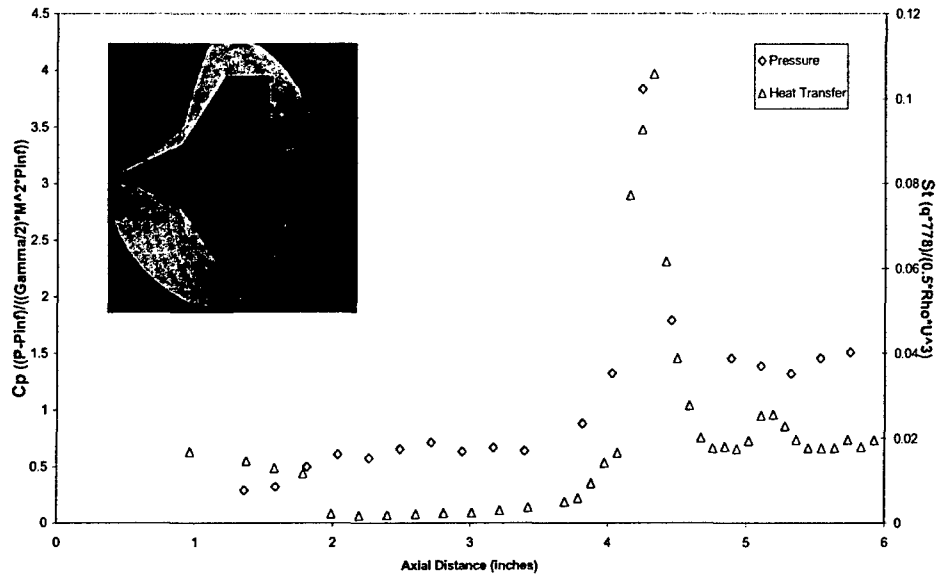


Figure 54 Schlieren Photograph and Measurement of Heat Transfer and Pressure for a 10 kft/s Air Flow

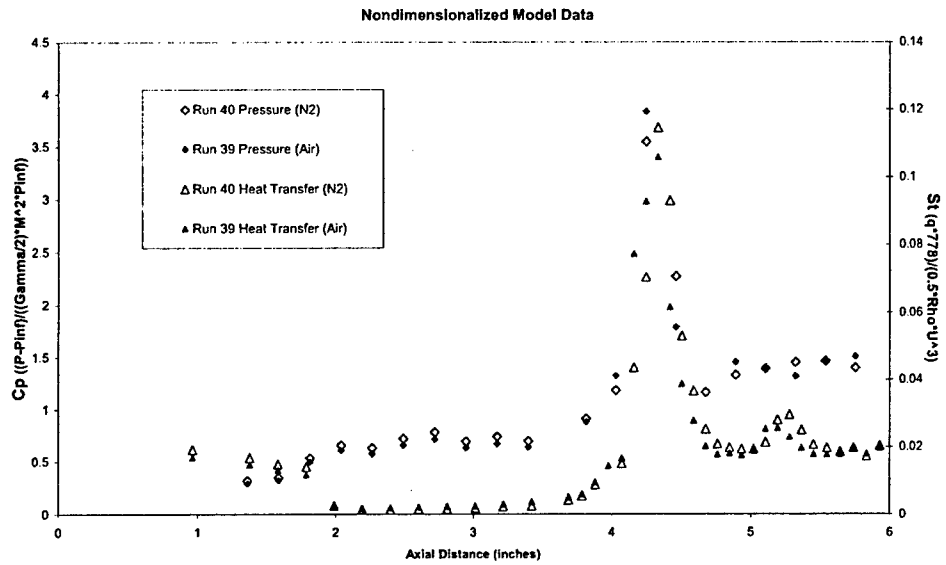


Figure 55 Comparisons between Measurements in Nitrogen and Air Flow at 10 kft/s

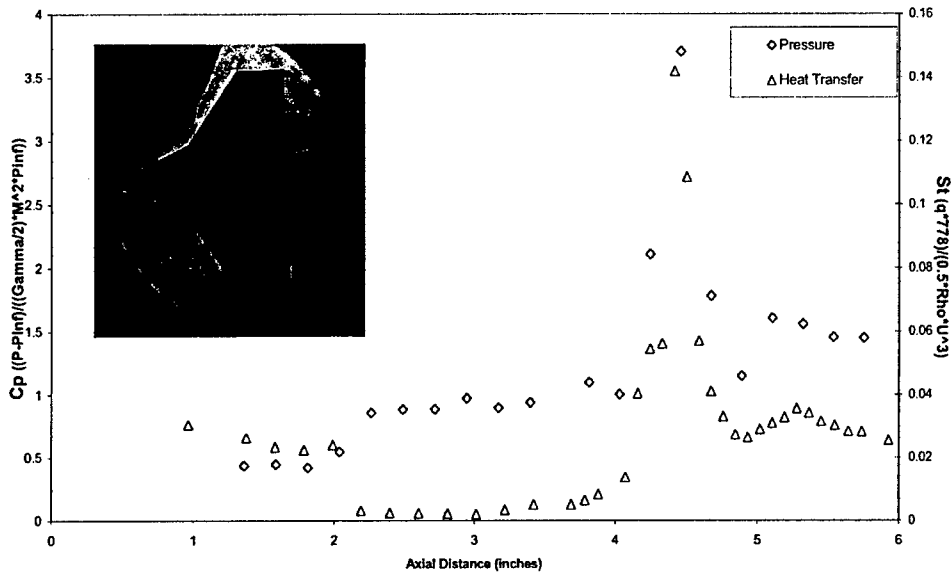


Figure 56 Schlieren Photograph and Measurement of Heat Transfer and Pressure for a 14 kft/s Nitrogen Flow

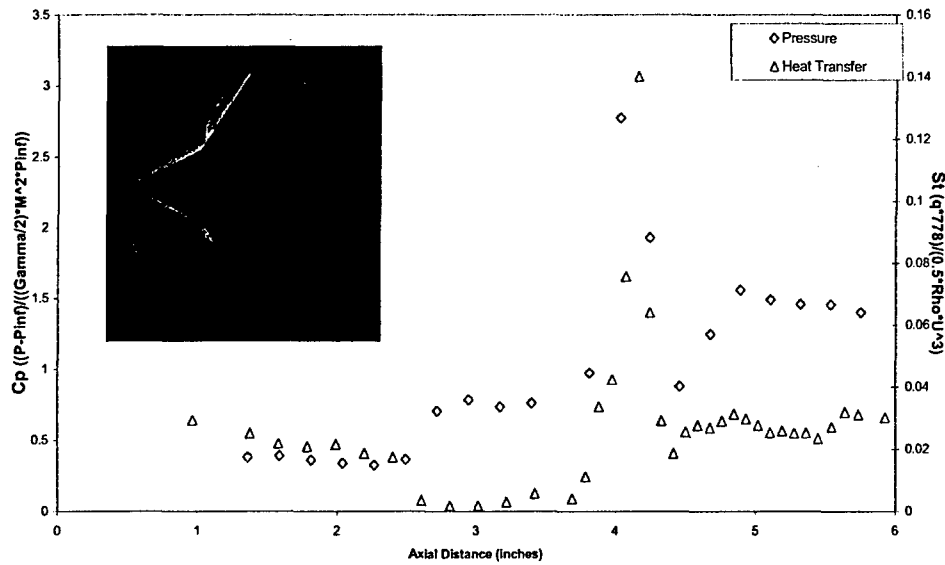


Figure 57 Schlieren Photograph and Measurement of Heat Transfer and Pressure for a 14 kft/s Air Flow

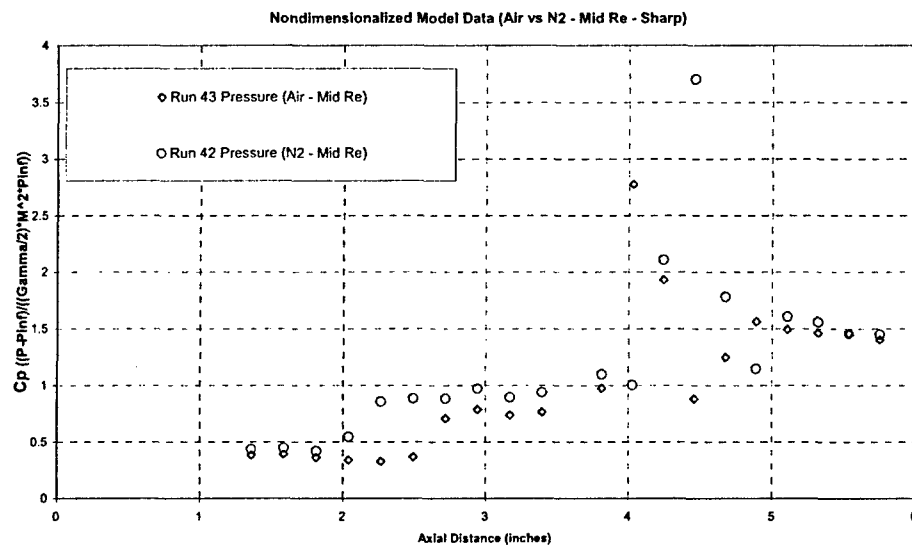


Figure 58 Comparisons between Pressure Measurements in Nitrogen and Air Flow at 14 kft/s

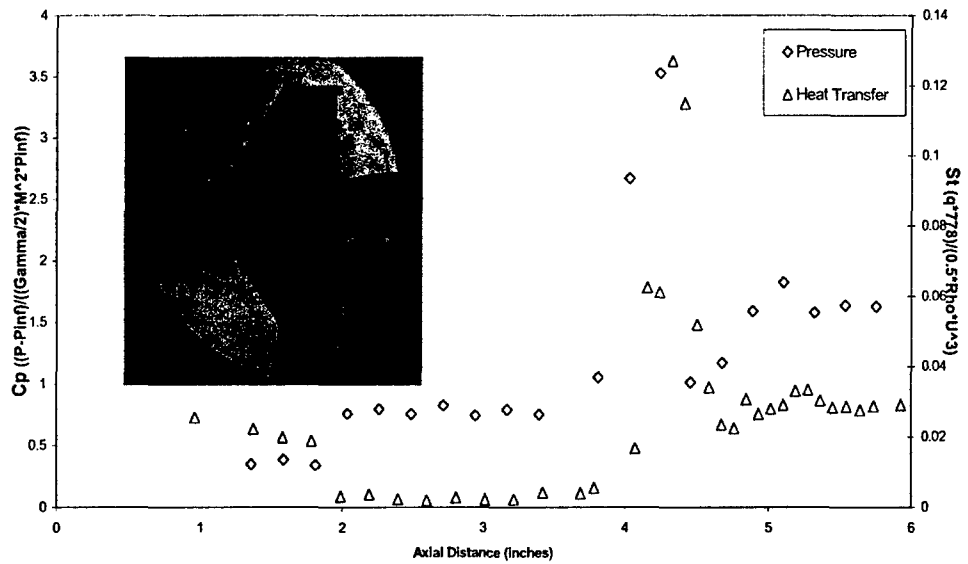


Figure 59 Schlieren Photograph and Measurement of Heat Transfer and Pressure for a 14 kft/s Nitrogen Flow at Higher Reynolds Number

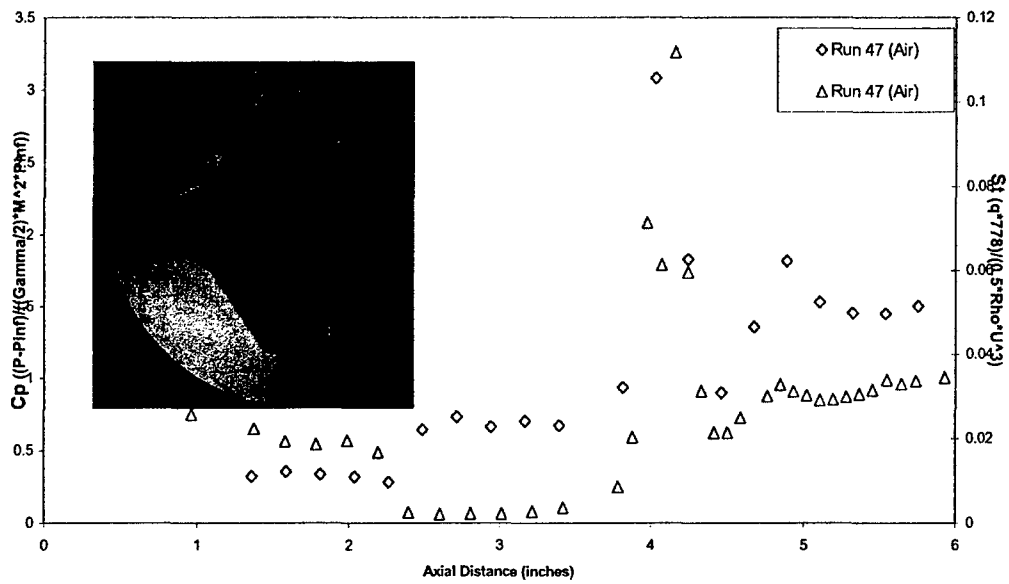


Figure 60 Schlieren Photograph and Measurement of Heat Transfer and Pressure for a 14 kft/s Air Flow at Higher Reynolds Number

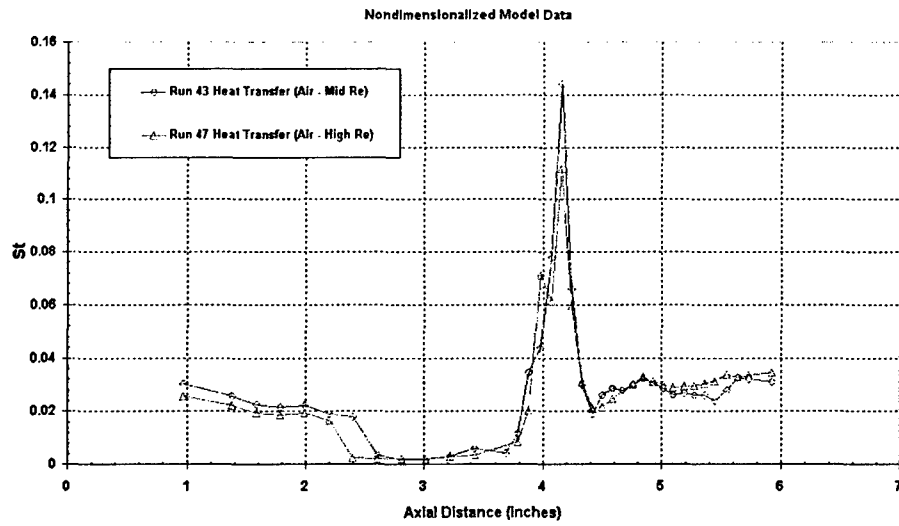


Figure 61 Correlations of Heat Transfer Measurements Obtained at Two Reynolds Number Conditions in Air Flow at 14 kft/s

MEASUREMENTS IN THE LENS X FACILITY ON DOUBLE CONE MODEL

Introduction

In the second phase of the experimental program to examine real gas effects over the double cone, preliminary studies were conducted during the development of the LENS X facility. A new double cone model was constructed for this phase of the program which contained more robust pressure and heat transfer instrumentation to withstand the potential damage from Mylar and metallic particles which occur in expansion tunnels. The model employed in this study is shown in Figure 62 and contains more robust coaxial heat transfer instrumentation. The location of the heat transfer and pressure instrumentation of this model is shown in Figure 63. As discussed earlier, the basic tunnel was highly instrumented to evaluate its performance during these studies; the survey rakes which were placed at the exit plane of the expansion tube were removed and the instrumentation used in a small rake placed above the model in the test section. Survey rake measurements indicated a test core of approximately 24 inches.

Measurements on the Double Cone Configuration in LENS X

The test conditions selected for these studies closely replicated those from earlier studies in the LENS I tunnel at velocities of 10 kft/s and 14 kft/s. A Schlieren photograph of the flow obtained in the LENS X facility is shown in Figure 64; we see flow patterns similar to those shown in Figure 56 obtained in LENS I. The heat transfer and pressure distributions obtained on the model in nitrogen at the higher velocity are shown in Figure 65. These distributions again closely replicate those obtained earlier in the LENS I facility where the separated region extends to within two inches of the sharp nosetip and the peak pressure and heat transfer region is approximately 4.5 inches from the leading edge. We plan to continue these studies during further development work in the LENS X facility. Numerical computations are being conducted to compare with the measurements in LENS X.

The results of this study are also presented in AIAA Paper 2004-0916.

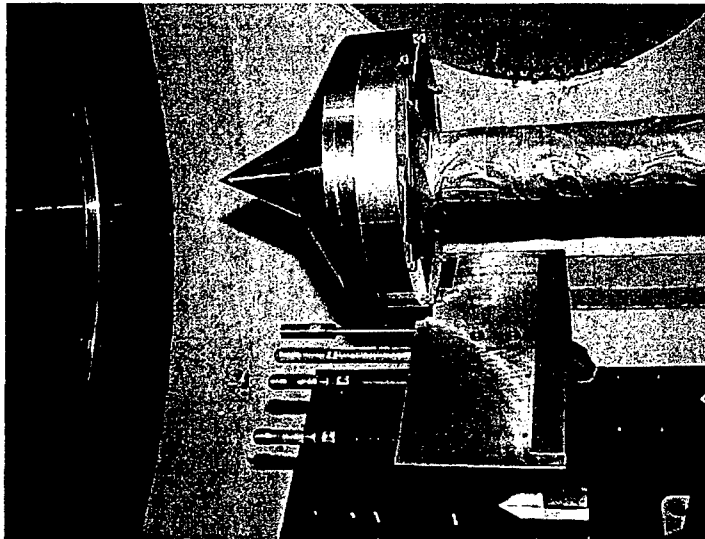


Figure 62 Double Cone Model used in LENS X Program

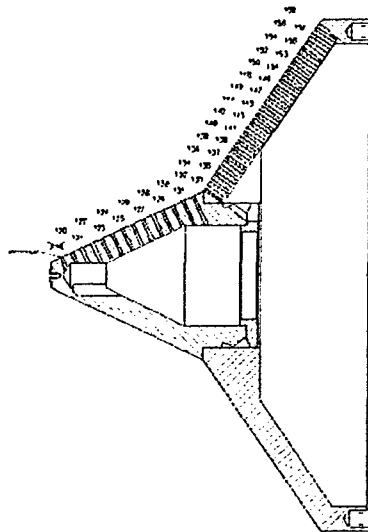


Figure 63 Location of Heat Transfer and Pressure Instrumentation on Double Cone Model for LENS X Studies

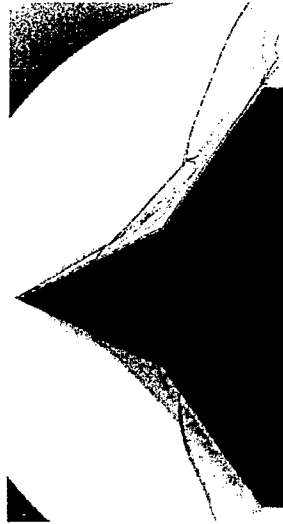


Figure 64 Schlieren Photograph Obtained in LENS X Studies and Comparison with Navier-Stokes Flowfield Predictions

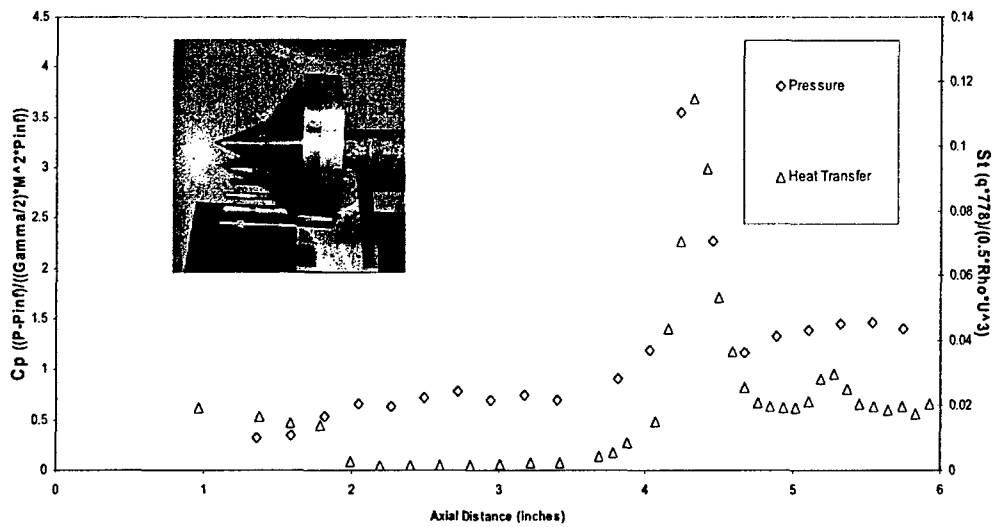


Figure 65 Heat Transfer and Pressure Measurements obtained in Nitrogen Flow at 14 kft/s

NAVIER-STOKES PREDICTIONS OF REAL GAS EFFECTS AND COMPARISON WITH EXPERIMENTS

Predictions with Navier-Stokes codes for comparison with the measurements for nitrogen and air flows over the double cone configuration have been made at the University of Minnesota by Graham Candler (Ref. 17) and at NASA Langley by Peter Gnoffo (Ref. 18). The freestream conditions were derived from tunnel measurements and numerical simulations.

Comparison between Candler's computations and measurements in the nitrogen flow over the double cone configuration are shown in Figure 66. The computations are in excellent agreement with experiment. Gnoffo's (Ref. 10) calculations for the same model configuration and freestream conditions are shown in Figure 67. These calculations slightly underpredict the size of the separated region, although pressure and heat transfer are in good agreement both upstream and downstream of the interaction region. Although peak pressure and heating levels are similar to those measured, this region occurs upstream of the measured values.

Comparison between measurements in air and Candler's calculations are shown in Figure 68. Although Candler's calculations are in close agreement with the heat transfer and pressure upstream and downstream of the interaction region, they underpredict the length of the separated region and significantly underpredict the peak heating in the reattachment/shock/shock interaction region. Gnoffo's predictions for air flow over the double cone shown in Figure 69. Again, they are in good agreement both upstream and downstream of the interaction region, however they also poorly predict the length of the separated region and the heating levels in the reattachment/shock/shock interaction region. It is clear that the structure of the recompression process is markedly different between experiment and the two sets of predictions and thus it is not surprising that the length of the separated region is poorly predicted. These results suggest that future experimental and numerical studies should focus on investigating the difference in flow structure in the recompression region which results from real gas effects.

The results of this study are also presented in AIAA Paper 2003-3641.

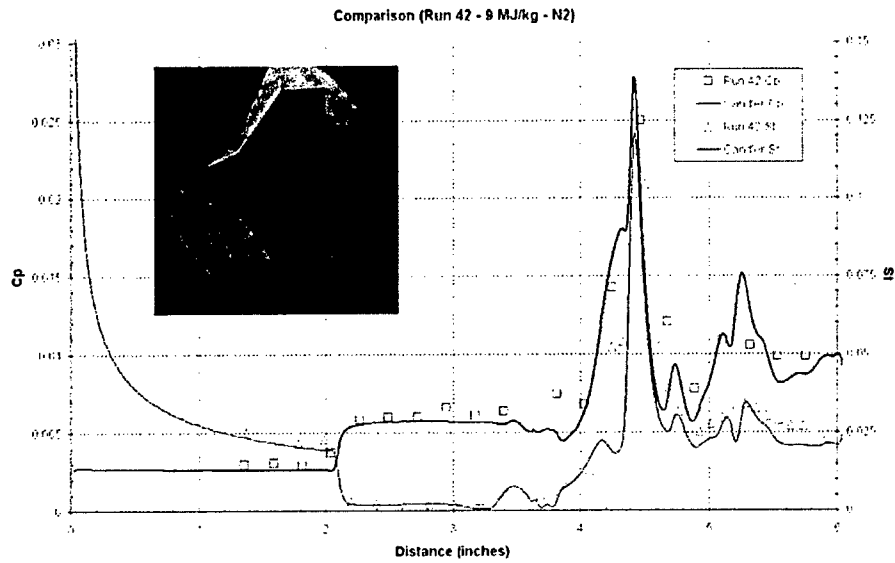


Figure 66 Comparison between Heat Transfer and Pressure Measurements in Nitrogen at 14 kft/s and Navier-Stokes Calculations by Candler

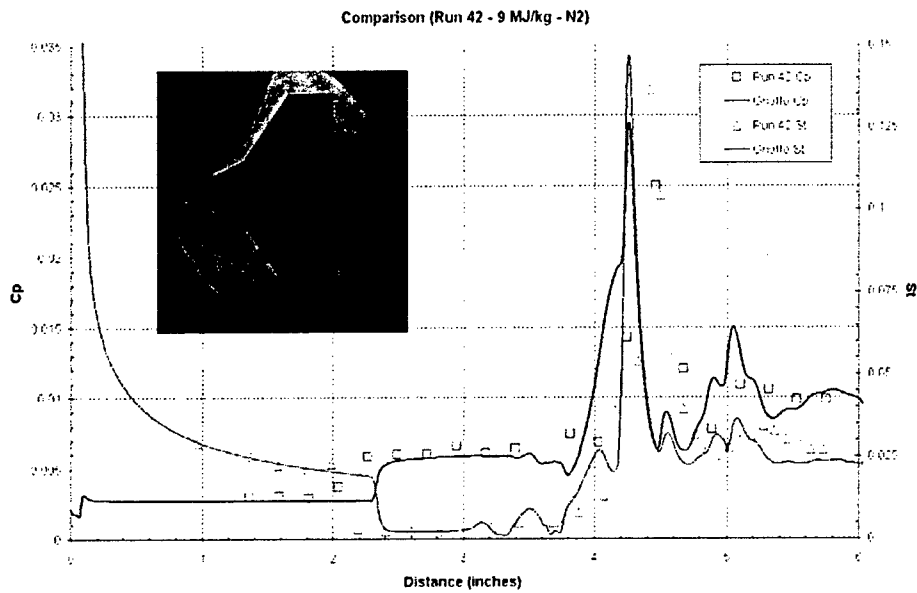


Figure 67 Comparison between Heat Transfer and Pressure Measurements in Nitrogen at 14 kft/s and DSMC Calculations by Gnoffo

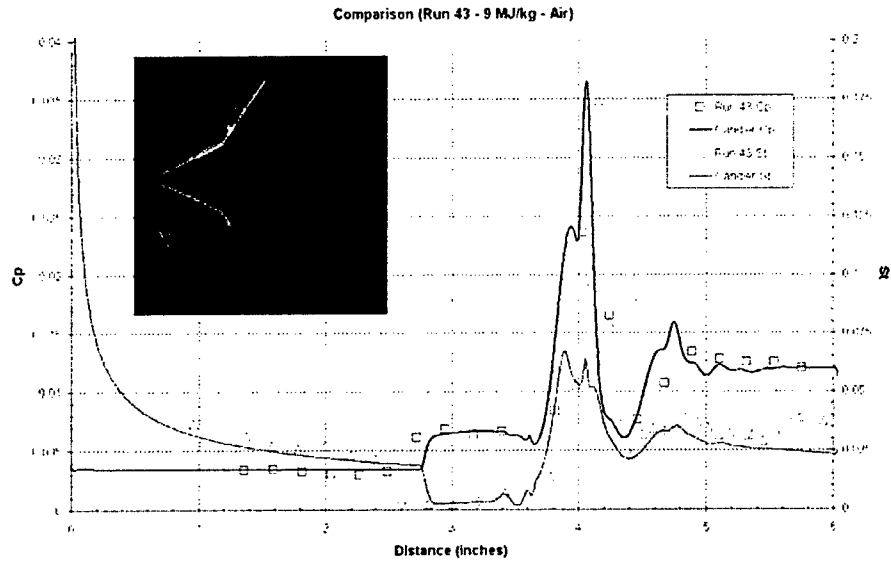


Figure 68 Comparison between Heat Transfer and Pressure Measurements in Air at 14 kft/s and Navier-Stokes Calculations by Candler

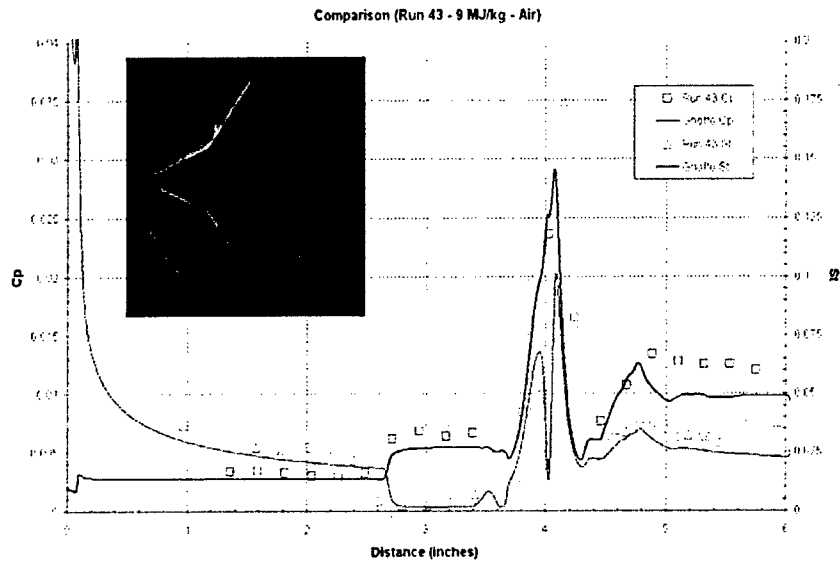


Figure 69 Comparison between Heat Transfer and Pressure Measurements in Air at 14 kft/s and DSMC Calculations by Gnoffo

PRELIMINARY RESULTS OF STUDIES OF REAL GAS EFFECTS ON REGIONS OF VISCOUS/INVISCID INTERACTION ON A NASA SPACE SHUTTLE CONFIGURATION

Introduction

As discussed in the introduction of this report, real gas effects have been shown in flight to play a significant role in controlling the stability and aerothermal loads of vehicles traveling at velocities of 12,000 ft/s and above. As also demonstrated on the double cone configuration, real gas effects can influence the size and properties of regions of viscous interaction in both separated and unseparated interaction regions. Although there have been a number of numerical computations and indirect experimental investigations, there have not been definitive coupled experimental and theoretical studies that have completely explained the differences between the pitching moments measured in ideal gas facilities and the measurements obtained in flight on the space shuttle. Our experimental program to investigate the "pitching moment anomaly" builds on the experimental and theoretical studies of the flow over the double cone configuration where regions of shock wave/boundary layer interaction similar to those over the shuttle flap were developed at the cone/cone junction. As in the earlier studies, the shuttle experiments were designed to obtain measurements in air and nitrogen over a range of freestream enthalpies spanning the regime from perfect gas to a flow with significant oxygen dissociation in stagnation regions and regions of separated flow at the flap/body junction. At the beginning of these studies the measurements were made over a range of Reynolds numbers to determine the Reynolds numbers below which the flow remained fully laminar over the flap. Measurements were also made for several flap angles, again seeking conditions where the flow remained fully laminar so that the influence of real gas effects could be assessed in a laminar flow where solutions for the Navier-Stokes equations could reasonably be expected to be accurate.

Models, Instrumentation and Test Conditions Employed in the Experimental Studies

We employed a 1.8% scale model of the space shuttle which was constructed by CUBRC to investigate the application of temperature-sensitive paint and Macor inserts to accurately measure the local and spatial heating rates around the leading edge of the shuttle. This model shown in Figure 70a and b was constructed from aluminum. For this study, we added stainless steel inserts along the centerline of the shuttle and on an outer ray where we believed real gas effects could significantly influence the static pressure in regions of positive pressure gradient. Because of the harsh environment at which these studies were conducted, we mainly employed coaxial thermocouple gages to measure heat transfer rate, although as illustrated in Figure 70c, a number of thin film gages were installed principally to provide a secondary calibration and check on the accuracy of the thermocouple gages. We employed both piezoelectric (PCB) and piezoresistive (Endevco) high frequency pressure transducers in the model as also shown in Figure 70c.

The experimental studies were conducted in the LENS I tunnel equipped with the D nozzle to generate flows with velocities from 3,000 to 16,000 ft/s. The tests were conducted with the model at incidence angles of 40° and 50° with flap angles of 13° and 17°. The unit Reynolds numbers at which the tests were conducted varied from $4.5E^4/\text{ft}$ to $0.2E^6/\text{ft}$.

Results and Discussions

The complete analysis of the experimental results and comparisons with numerical prediction methods remains to be completed. However, here we will summarize the major results obtained

in this study; a complete reporting including numerical comparisons will be presented at the forthcoming annual AIAA meeting.

As discussed earlier, the initial studies with the shuttle configuration were designed to select Reynolds number conditions at which the flow remained fully laminar over the flap. These studies were conducted over a range of freestream enthalpies to investigate the effects of real gas chemistry on transition as well as to ensure that test cases involving fully laminar flows could be selected. A typical set of heat transfer measurements along the centerline of the shuttle model for a range of unit Reynolds numbers of the freestream are shown in Figure 71. This data is plotted in nondimensional form to illustrate the deviation of flap heating from the laminar level when transition occurs at the larger Reynolds number. These measurements illustrate that transition in the separated region over the flap occurs at extremely low Reynolds numbers and when it occurs, the heating levels increase significantly from the laminar level. A second set of measurements at a higher enthalpy illustrates as discussed above that transition was observed to occur over the flap at lower Reynolds numbers in the high enthalpy flows. This latter conclusion is of significant importance in using measurements obtained in cold facilities to predict the aerothermal characteristics associated with flight. The measurements shown in Figure 72 made in high enthalpy flows in the separated region at the body/flap junction illustrate how the heat transfer increases significantly over the flap and the separated region shortened when transition occurs in the separated shear layer. Also as shown in Figure 72b, the high pressure region on the flap is extended when transition occurs making the flap more effective. As illustrated in the heat transfer results the flow of nondimensional heat transfer to the flap does not differ significantly at Reynolds numbers of 6×10^4 and 4.5×10^4 indicating that the flow remains fully laminar under these conditions. We followed the studies of Reynolds number effects with sets of measurements in air and nitrogen to investigate real gas effects.

Shown in Figure 73 are heat transfer measurements close to the body/flap junction obtained in high enthalpy flow in air and nitrogen for the two Reynolds numbers where the flow remains fully laminar over the flap. Here we observe that the separated region decreases in length when high temperature nonequilibrium air is employed in the test flow rather than nitrogen.

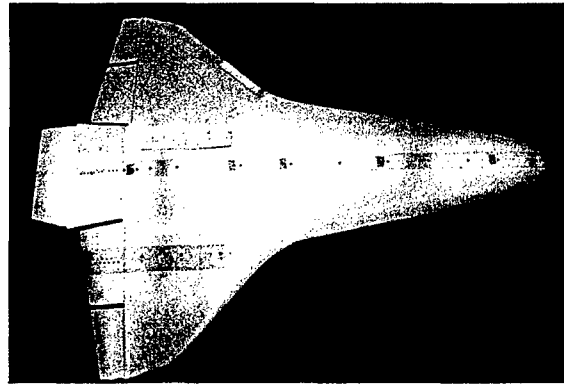
We then made measurements in air for a range of total enthalpies at a single Reynolds number of 6×10^4 . As illustrated in Figure 74, we observed that the separated region decreased in size as the freestream enthalpy was increased from 3 MJ/kg where real gas effects are small to 9.5 MJ/kg where significant oxygen dissociation occurs in the separated recirculation region. These results are consistent with the findings from the studies with the double cone configuration and suggest that real gas effects would increase flap effectiveness and increase pitching moment.

The sets of measurements obtained with the outer ray of instrumentation do support the contention that real gas effects contribute to a lowering of the pressure in the expansion region thereby lowering the pitching moment; and since there is an extensive area over which this effect occurs, it is this effect that contributes to the pitching moment anomaly observed in flight. Examples of the measurements along the outer ray are shown in Figure 75 illustrating decreased levels with increasing enthalpy of real gas effects. Again, switching from nitrogen to air has a similar effect.

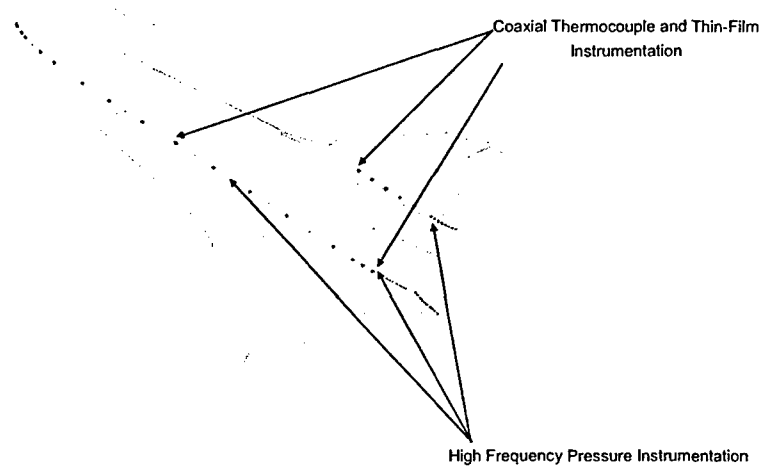
During the remainder of the year we expect to perform detailed numerical computations to compare with this data set and that obtained on the double cone configuration. *These data sets will be provided to support a code validation activity organized in conjunction with AFOSR.*



(a)



(b)



(c)

Figure 70 Model and Instrumentation for Real Gas Studies over Shuttle Configuration in LENS Tunnels

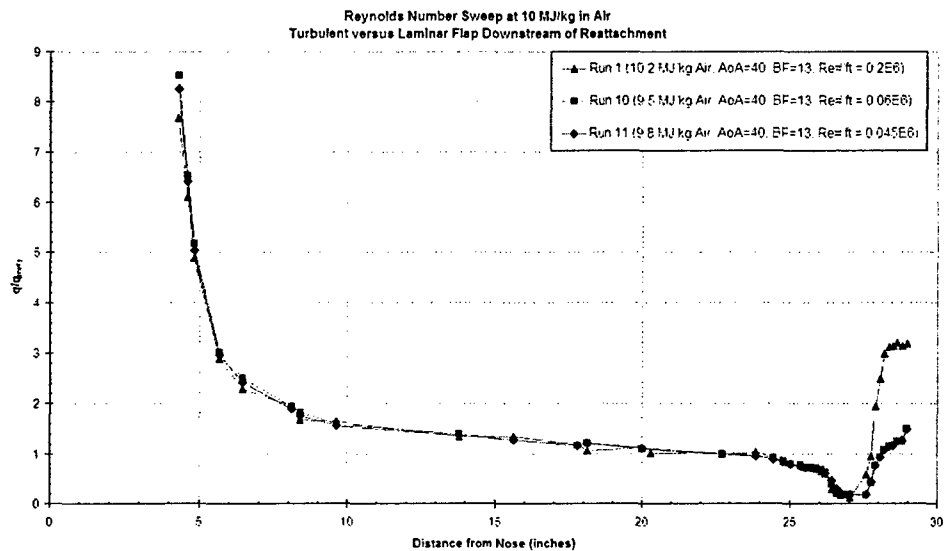


Figure 71 Centerline Heat Transfer Reynolds Number Sweep Illustrating Laminar and Turbulent Heating Downstream of Reattachment

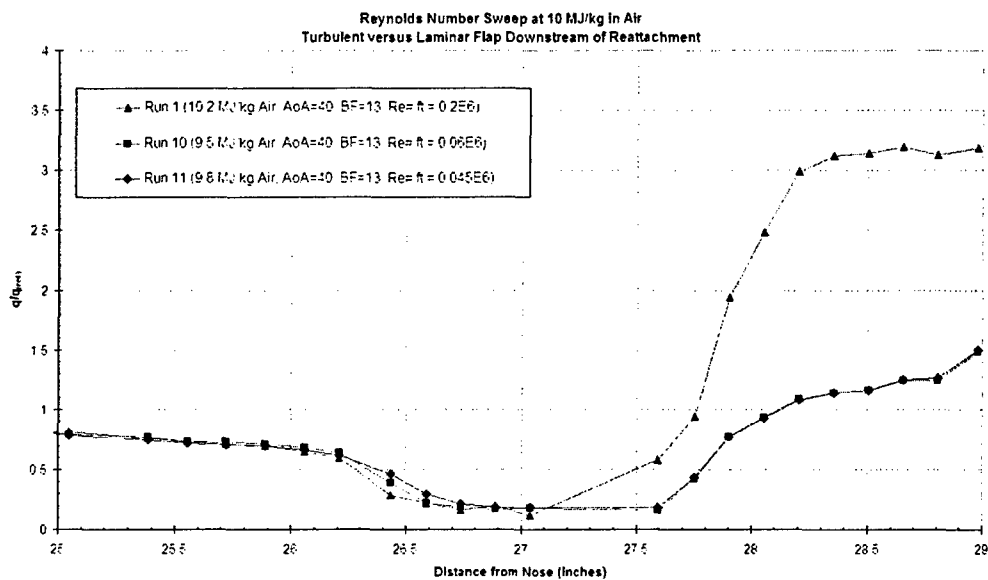


Figure 72a Flap/Body Junction Heat Transfer Reynolds Number Sweep Illustrating Laminar and Turbulent Heating Downstream of Reattachment

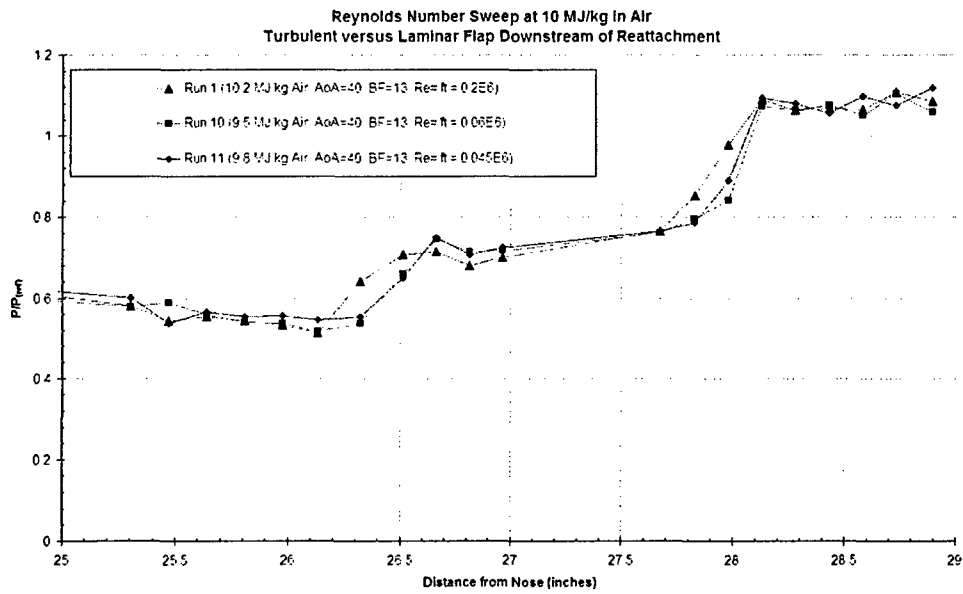


Figure 72b Flap/Body Junction Pressure Reynolds Number Sweep Illustrating Laminar and Turbulent Heating Downstream of Reattachment

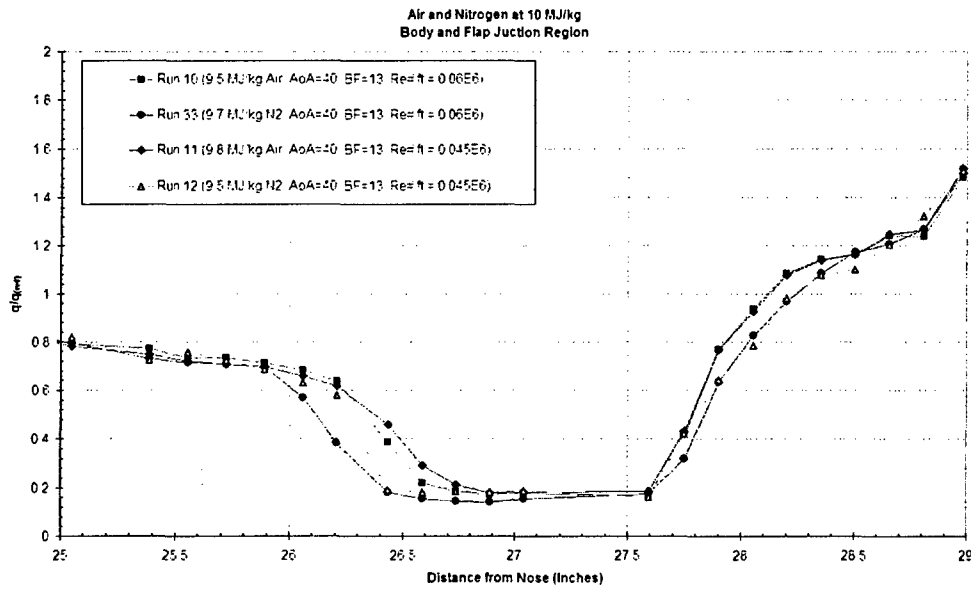


Figure 73 Flap/Body Junction Heat Transfer in High Enthalpy Air and Nitrogen Flows

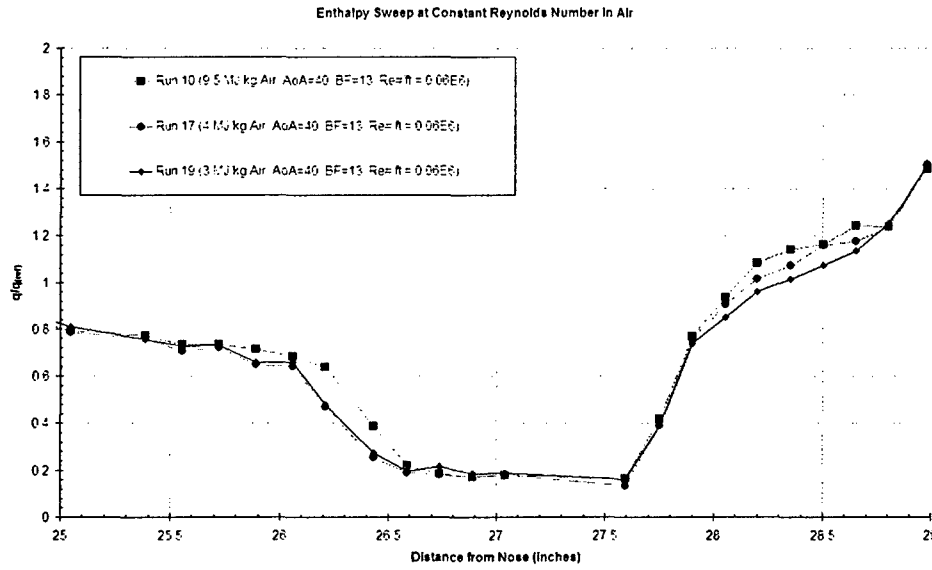


Figure 74 Flap/Body Junction Heat Transfer over Range of Enthalpies in Air at Constant Reynolds Number

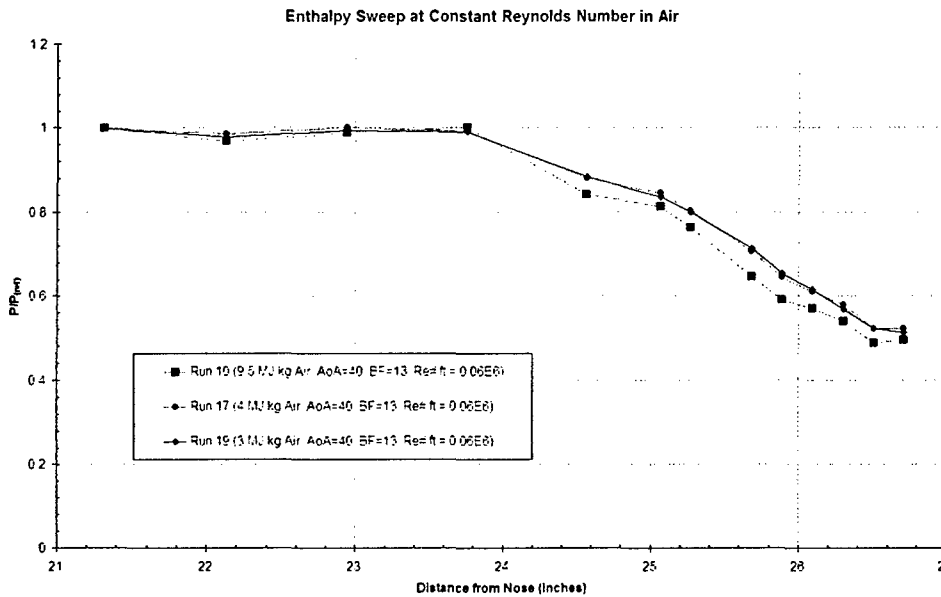


Figure 75 Pressure Measurements made on Orbiter Wing Acreage over a Range of Enthalpies in Air at Constant Reynolds Number

CONCLUSIONS

Experimental studies coupled with numerical simulations were performed to examine the effects of low density flows and real gas effects on the aerothermal characteristics of the flows in the LENS I shock tunnel and LENS X expansion tunnel and on simple and complex flowfields developed in hypervelocity flows over simple and complex vehicle configurations. Measurements with hollow cylinder/flare and double cone configurations were obtained over a range of Reynolds numbers and Mach numbers to evaluate the performance of modified Navier-Stokes and DSMC methods. These studies demonstrated that in the absence of real gas effects the DSMC and Navier-Stokes solutions accounting for slip effects were in excellent agreement with the measurements. An extensive series of calibration and validation studies were performed to define the freestream flows in the LENS I and LENS X tunnels for low density flows and high enthalpy flows at velocities up to 16,000 ft/s. A major study was also successfully conducted to employ laser diagnostics to measure the velocity and concentration of NO and oxygen in the freestream. Measurements made in these studies indicated while the velocity was accurately predicted by the numerical code, the levels of NO concentration (2% to 3%) were significantly less than those predicted by the Navier Stokes codes (~6%).

The measurements on the double cone configuration in air and nitrogen flows demonstrated that while there was little effect of real gas chemistry on the structure of the interaction regions at velocities below 10,000 ft/s, at velocities above 13,000 ft/s there were significant differences between the interaction regions in nitrogen and air flows and while the computations agreed with the measurements in nitrogen, they differed significantly both in the size and properties of the interaction regions in air. These studies with the double cone configuration were followed by a major experimental program to evaluate real gas effects over a shuttle configuration with particular emphasis on the separated regions of shock wave/boundary layer interaction on the control surfaces and the expansion regions over the rear surfaces of the shuttle. These studies again demonstrated that real gas effects decrease the size of the interaction region over the flap control surface increasing its effectiveness while causing the pressures on the adjacent curved section of the wing to be lower because of nonequilibrium effects in the freestream. In these studies it was also observed that real gas chemistry can have a significant destabilizing effect on boundary layer transition resulting in real gas flows which become transitional or turbulent at lower Reynolds numbers than observed for flows in the absence of chemistry.

References

1. Maus, J.R., Griffith, B.J. Szema, K.Y., and Best, J.T., "Hypersonic Mach Number and Real Gas Effects on Space Shuttle Orbiter Aerodynamics," *J. of Space and Rockets*, Vol. 21, March-April 1984, pp. 136-141.
2. Holden, Michael S., Wadhams, Timothy P., Smolinski, Gregory J., Parker, Ronald A. and Harvey, John K., "Experimental Studies of Shock Interaction Phenomena associated with Hypersonic Airbreathing Propulsion," CUBRC Final Report 3640-1, January 31, 2002.
3. Holden, Michael S., Wadhams, Timothy P., and Candler, Graham V., "Experimental Studies in the LENS Shock Tunnel and Expansion Tunnel to Examine Real-Gas Effects in Hypervelocity Flows," AIAA 2004-0916, 42nd. AIAA Aerospace Sciences Meeting and Exhibit, Reno, NV, January 5-8, 2004.
4. Candler, G.V. and Nompelis, I., "CFD Validation for Hypersonic Flight: Real Gas Flows," AIAA Paper 2002-0434, presented at the AIAA 40th. Aerospace Sciences Meeting and Exhibit, Reno, NV, January 14-17, 2002.
5. Large Energy National Shock Tunnels – Description and Capabilities, April 2004
6. Holden, M.S., Parker, R.A. "Lens Hypervelocity Tunnels and Application to Vehicle Testing at Duplicated Flight Conditions", Chapter 4, *Advanced Hypersonic Test Facilities*, Editors Frank Lu and Dan Marren, Volume 198, 2002
7. Dornheim, M. A., "Planetary Flight Surge Faces Budget Realities," *Aviation Week and Space Technology*, Vol. 145, No. 24, 9 Dec. 1996, pp. 44-46.
8. Parker, R., Wakeman, T., Holden, M., and MacLean, M., "Measuring NO Freestream Concentration Using Quantum Cascade Lasers at CUBRC," AIAA Paper 2006-0926, 44th. Annual Sciences Meeting & Exhibit, Reno, NV, 9-12 January 2006.
9. Nompelis, I., Candler, G., Holden, M. and Wadhams, T., "Real Gas Effects on Hypersonic Shock Wave Laminar Boundary Layer Interactions," AIAA 2003-0443, 41st. Aerospace Sciences Meeting and Exhibit, Reno, NV, January 6-9, 2003.
10. Candler, G.V., Nompelis, I., Druguet, M-C, Boyd, I.D., Wang, W-L, Holden, M.S., Wadhams, T.P., "CFD Validation for Hypersonic Flight: Hypersonic Double-Cone Flow Simulations," AIAA 2002-0581, presented at 40th Aerospace Sciences Meeting & Exhibit, January Reno, NV, January 13-17, 2002.
11. Markelov, G.N., Private Communication, 2003
12. Boyd, Iain, Private Communication, 2003
13. Moss, James, Private Communication, 2003.
14. Wright, M.J., Bose, D., and Candler, G.V., "A Data Parallel Line Relaxation Method for the Navier-Stokes Equations," *AIAA Journal*, Vol. 36. No. 9, pp 1603-1609, September 1998.
15. Hollis, B., Liechty, D.S., Wright, M.W., Holden, M.S, Wadhams, T.P., MacLean, M. and Dyakonov, A., "Transition Onset Correlations and Turbulent Heating Measurements for Mars Science Laboratory Entry Vehicle," AIAA Paper 2005-1437, 43rd. AIAA Aerospace Meeting and Exhibit, Reno, NV, January 10-13, 2005
16. MacLean, M., and Holden, M., "Catalytic Effects of Heat Transfer Measurements for Aerothermal Studies with CO₂," AIAA Paper 2006-0182, 44th. Annual Sciences Meeting & Exhibit, Reno, NV, 9-12 January 2000
17. Candler, Graham V., Private Communication, 2003
18. Gnoffo, Peter, Private Communication, 2003
19. Holden, M.S., Bergman, R.C., Harvey, J.K., Boyd, I.D. and George, J., "Experimental Studies of Real-Gas Effects over a Blunted Cone/Flare Configuration in Hypervelocity Airflows," AIAA 97-0855, presented at the 35th. Aerospace Sciences Meeting and Exhibit, Reno, NV, January 6-10, 1997.

20. Holden, M.S., "Real Gas Effects on Regions of Viscous-Inviscid Interaction in Hypersonic Flows," AIAA 97-2056, 28th AIAA Fluid Dynamics Conference, 4th AIAA Shear Flow Control Conference, Snowmass Village, CO, June 29-July 2, 1997.